Naval Research Laboratory

Washington, DC 20375-5320

NRL/MR/7221--95-7678

NRL Volume Imaging Lidar and Its Capabilities

JEFFREY E. JAMES
WILLIAM P. HOOPER

Remote Sensing Physics Branch
Remote Sensing Division

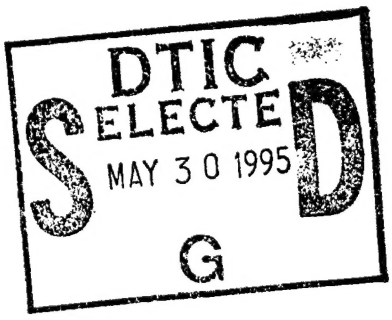

May 31, 1995

REPORT DOCUMENTATION PAGE

Form Approved
OMB No. 0704-0188

1. AGENCY USE ONLY (*Leave Blank*)	2. REPORT DATE	3. REPORT TYPE AND DATES COVERED
	May 31, 1995	

4. TITLE AND SUBTITLE

NRL Volume Imaging Lidar and Its Capabilities

5. FUNDING NUMBERS

PE - 61153N
PR - LR0310341

6. AUTHOR(S)

Jeffrey James and William P. Hooper

7. PERFORMING ORGANIZATION NAME(S) AND ADDRESS(ES)

Naval Research Laboratory
Washington, DC 20375-5320

8. PERFORMING ORGANIZATION REPORT NUMBER

NRL/MR/7221--95-7678

9. SPONSORING/MONITORING AGENCY NAME(S) AND ADDRESS(ES)

Office of Naval Research
Arlington, VA 22217-5000

10. SPONSORING/MONITORING AGENCY REPORT NUMBER

11. SUPPLEMENTARY NOTES

12a. DISTRIBUTION/AVAILABILITY STATEMENT

Approved for public release; distribution unlimited.

12b. DISTRIBUTION CODE

13. ABSTRACT (*Maximum 200 words*)

A volume imaging lidar (VIL) has been designed at the Naval Research Laboratory (NRL) to characterize large (10 m to 1 km) aerosol structures in the maritime environment. The system is mounted in a shipping container and uses a dual mirror scanning system, Nd:YAG (1.06 micron) laser, and a 35 cm telescope. Measurements are routinely made at NRL's Chesapeake Beach Detachment (CBD) located 40 miles southeast of Washington DC. In addition, the system has been used at coastal sites (Wallops Island, VA and Point Sur, CA) and aboard ship (RV GLORITA). This paper discusses the design and operation of the VIL as well as its unique measurement capabilities.

14. SUBJECT TERMS

Lidar	Aerosol	Laser radar
Volume imaging	Atmospheric measurements	Aureole lidar extinction
VIL	Wind speed	Backscatter
Scanning lidar	Turbulence	

15. NUMBER OF PAGES

71

16. PRICE CODE

17. SECURITY CLASSIFICATION OF REPORT	18. SECURITY CLASSIFICATION OF THIS PAGE	19. SECURITY CLASSIFICATION OF ABSTRACT	20. LIMITATION OF ABSTRACT
UNCLASSIFIED	UNCLASSIFIED	UNCLASSIFIED	UL

NSN 7540-01-280-5500

Standard Form 298 (Rev. 2-89)
Prescribed by ANSI Std 239-18
298-102

TABLE OF CONTENTS

NRL VOLUME IMAGING LIDAR AND ITS CAPABILITIES

1. History of Lidar

Lidar (which stands for "light detection and ranging") is the optical equivalent of radar. It was developed shortly after the invention of the laser and the development of Q-switching.[1] Q-switching is a method of releasing the laser's energy over a very short period of time, creating a short pulse of laser light with a duration in the range of 10-100 nsec. A lidar transmits pulses of laser light into the atmosphere and measures the amount of light elastically scattered by aerosols back towards the transmitter. A receiver, generally a telescope, is located with the transmitter and looks at a narrow field of view in the same direction that the laser is pointed. The backscattered light entering the receiver is focused onto an optical sensor (typically a photodiode or photomultiplier tube (PMT), the analog signal from the sensor is then analyzed, statistically processed, and displayed graphically on a color monitor using a false-color scale to indicate the magnitude of the return. By knowing the time at which the laser pulse originates from the transmitter and the time the scattered light reaches the receiver, a range resolved signal can be obtained.

The lidar has many uses including the study of the atmosphere and its characteristics, the realtime study of cloud structures and their formation, aerosol generation, ship tracking and the capability to provide wind and turbulence measurements over a wide area.

2. Lidar Theory

The signal strength, $P(\phi_i,\theta_i,R_j,t_i)$, returned (backscattered) from a laser beam propagating through the atmosphere for a monostatic lidar scanning in azimuth and elevation is given by[2]:

$$P(\phi_i,\theta_i,R_j,t_i)=\frac{K\beta(\phi_i,\theta_i,R_j,t_i)\exp[-2\tau(\phi_i,\theta_i,R_j,t_i)]}{R_j^2}+n'(\phi_i,\theta_i,R_j,t_i) \qquad (1)$$

where

- i is the waveform number in a series of returns,
- j is the range bin number,
- t_i is time,
- R_j is the radial distance along the propagation path,
- θ_i is the elevation scan angle,
- ϕ_i is the azimuth scan angle,

Manuscript approved February 9, 1995.

K are system constants

β is the volume backscatter coefficient,

τ is optical depth and

n' is the sum of all noise sources.

Note: The noise term represents the sum of sky and electronic noise and as a time series is assumed at any given range to have a zero mean.

Since a logarithmic amplifier is used, the digitized, range corrected signal from the amplifier is given by

$$S(\phi_i,\theta_i,R_j,t_i)=\log_a[R_j^2 P(\phi_i,\theta_i,R_j,t_i)]=$$

$$\log_a[K]+\log_a[\beta(\phi_i,\theta_i,R_j,t_i)]-\frac{2\tau(\phi_i,\theta_i,R_j,t_i)}{\ln[a]}+\log_a[1+n(\phi_i,\theta_i,R_j,t_i)]\ , \qquad (2)$$

where

S = the corrected waveform,

a = the logarithmic base of the amplifier and,

n = noise (scaled by the signal strength).

Unlike the noise term, n', in equation (1), n is scaled by the return signal and therefore is range dependent. Since the noise term is scaled by the signal component, it can be statistically characterized by a signal to noise ratio, see appendix 1. If a convex hull[3] is used to find a minimum function, the equation becomes:

$$S_o(\phi_i,\theta_i,R_j,t_i)=conv(S(\phi_i,\theta_i,R_j,t_i))=$$

$$\log_a[K]+\log_a[\beta_o(\phi_i,\theta_i,R_j,t_i)]-\frac{2\bar{\tau}(\phi_i,\theta_i,R_j,t_i)}{\ln[a]}+\log_a[1+n_o(\phi_i,\theta_i,R_j,t_i)] \qquad (3)$$

where *conv* is used to denote the convex hull operation, subscript o denotes the minimum, β_o is the minimum volume backscatter, and $\bar{\tau}$ is the 'average' optical depth. For this analysis, convex hull is assumed to find a range-independent, minimum backscatter. Figure 1 shows an example of a lidar return and the associated minimum return found from the convex hull operation.

The difference between equations (2) and (3) is

$$S(\phi_i,\theta_i,R_j,t_i)-S_o(\phi_i,\theta_i,R_j,t_i)=\frac{\ln[\beta(\phi_i,\theta_i,R_j,t_i)/\beta_o(\phi_i,\theta_i,R_j,t_i)]}{\ln(a)}+\epsilon(\phi_i,\theta_i,R_j,t_i) \quad (4)$$

where ϵ is the error term which is a range-dependent function of the noise term and optical depth. Since $S(\phi_i,\theta_i,R_j,t_i)$ is measured and $S_o(\phi_i,\theta_i,R_j,t_i)$ can be determined, backscatter normalized by the minimum backscatter can be calculated as

$$\frac{\beta(\phi_i,\theta_i,R_j,t_i)}{\beta_o(\phi_i,\theta_i,R_j,t_i)}\approx\exp[(S(\phi_i,\theta_i,R_j,t_i)-S_o(\phi_i,\theta_i,R_j,t_i))\ln(a)] \quad (5)$$

where the error term is neglected. This parameter is then plotted and used to study the atmospheric-oceanic processes like aerosol transport and aerosol generation by breaking waves. Figure 2 shows a normalized backscatter (derived from figure 1) and figure 3 shows a false color image of normalized backscatter for a series of lidar returns.

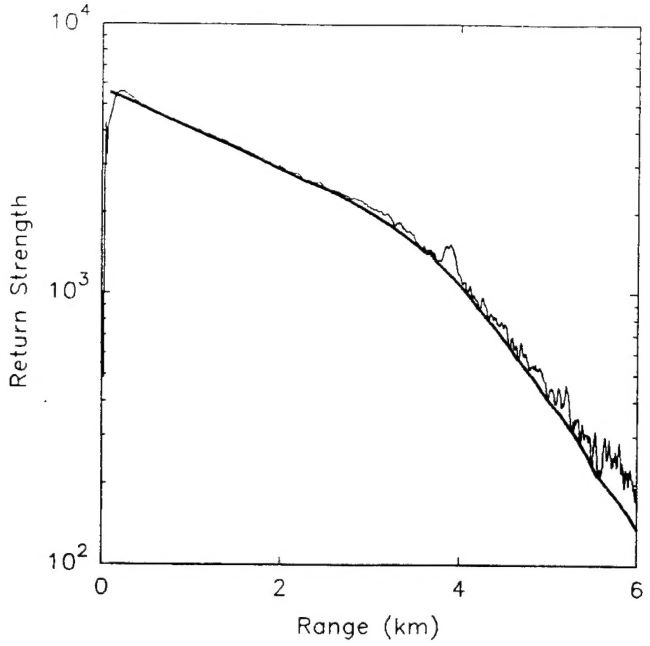

Figure 1. Profile from MAST (Monterey Area Ship Track) experiment (6/20/94 0724 PST). The upper curve (thin line) is the raw data. The lower curve (heavy line) is the minimum function generated from the convex hull operation. A plume from a commercial ship can be seen at 4 km.

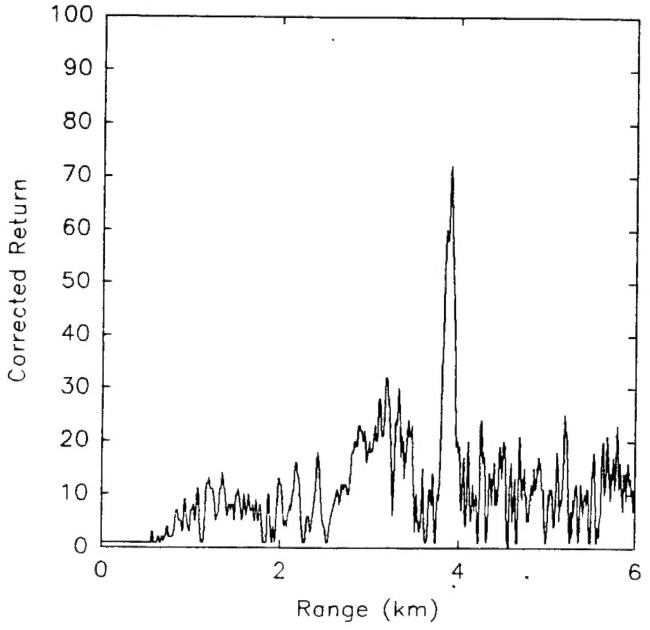

Figure 2. The normalized backscatter profiles generated for the curves shown in figure 1. The ship plume can again be seen at 4 km.

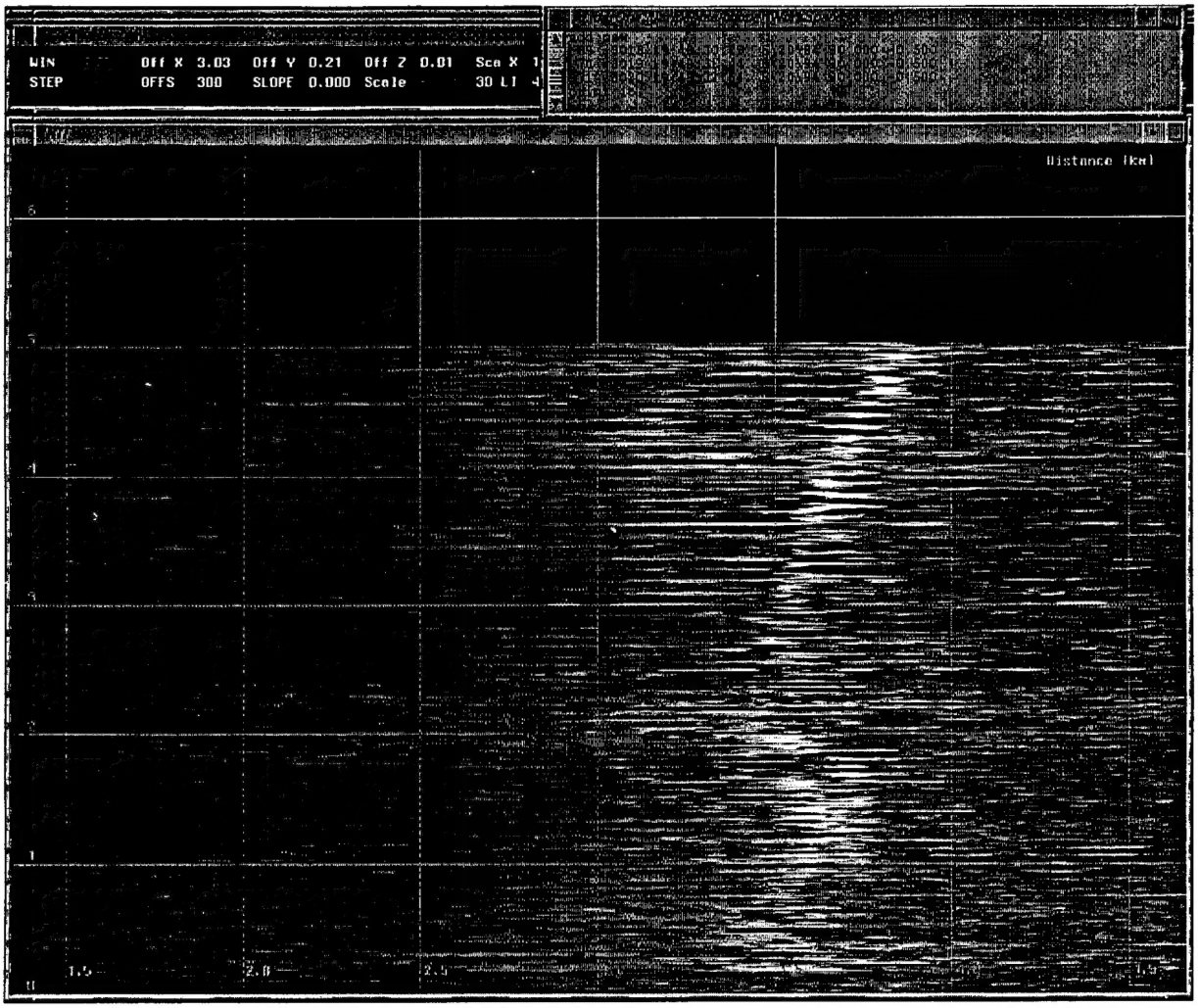

Figure 3. False color image of lidar RTI (range time indicator) is shown.

3. NRL Volume Imaging Lidar

The Naval Research Laboratory operates a volume imaging lidar (VIL) facility located at the Chesapeake Beach Detachment (CBD) approximately 40 miles southeast of Washington, DC, see figure 4. The VIL operates very much like the typical lidar described above but has the added capability to scan in both azimuth and elevation. The VIL can scan large-scale (1km^3) aerosol structures once per minute. Time-varying, 3-D images of clouds, sub-visible aerosol structures, sea spray and smoke plumes can be examined with this system. The targets are scanned by the lidar in a repetitive pattern and the return signal is stored, analyzed, and displayed in 3-D on a Silicon Graphics work station, all in realtime. Aerosol structures can be detected to a maximum range of 20 km with range resolution of 7.5 m.

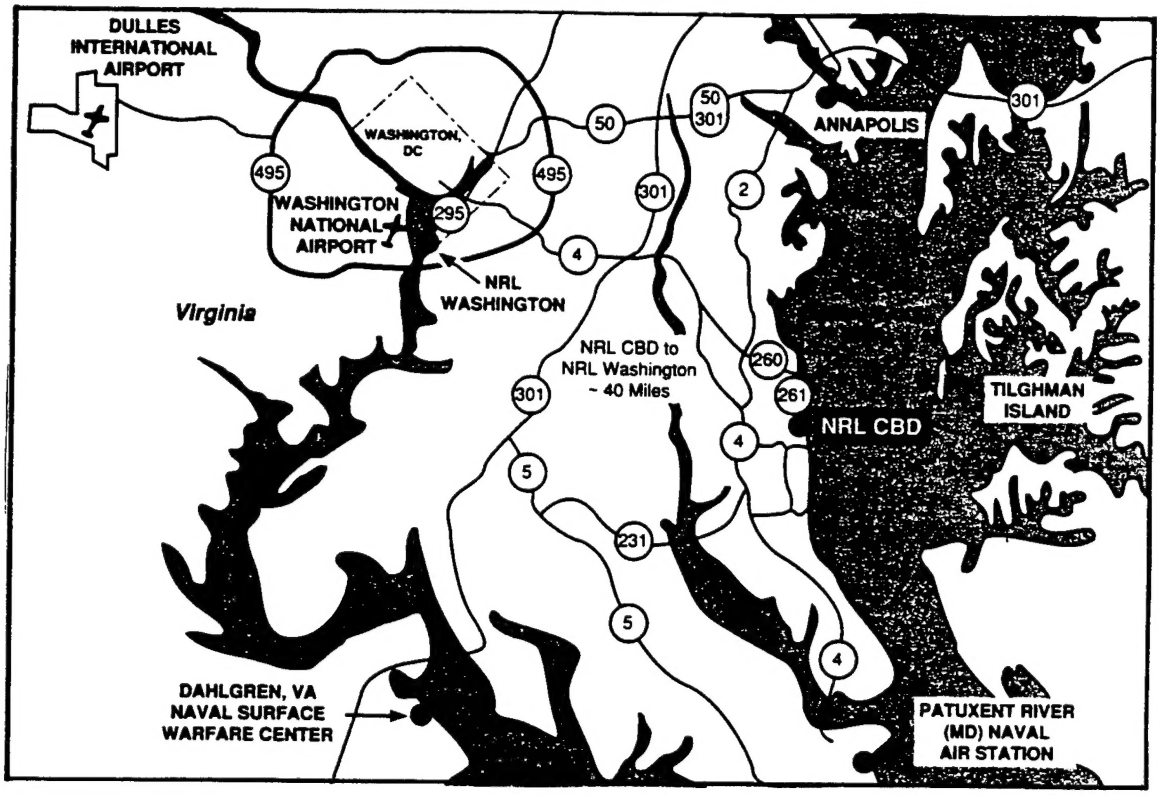

Figure 4. Location of CBD relative to the Naval Research Lab.

CBD is the principle field site for NRL lidar operations, testing and development. The VIL is maintained and operated at CBD unless it is participating in a field experiment. The operations site at CBD provides an excellent opportunity for lidar research. The VIL sits on top of a 30m cliff overlooking the Chesapeake Bay. The lidar has an unobstructed 160° view of the bay.

Sixteen kilometers directly across the bay from CBD is another NRL field site located on Tilghman Island. The Tilghman Island site has a 30m-tall tower located on the shoreline. The tower can be used as a target for aligning the VIL system optics. A retro-reflector is placed at the top of the tower and is used to reflect laser light from the VIL back towards the VIL site for calibration and alignment. A weather station operated by NOAA is located on Tilghman Island which can provide meteorological information for the coastal area. The zone between CBD and Tilghman Island has been approved as a laser firing range by the NRL Laser Safety Office. A sample of an outdoor laser-range firing-log can be found in appendix 2.

4. VIL Shelter Description

The VIL is housed in a 20′ by 8′ by 8′ aluminum shipping container that was modified by Oceaneering Technologies, Inc. and personnel at NRL, see figure 5. Modifications include electrical wiring, cooling and heating, plumbing and a rectangular hole in the roof for the scanning mechanism to pass through.

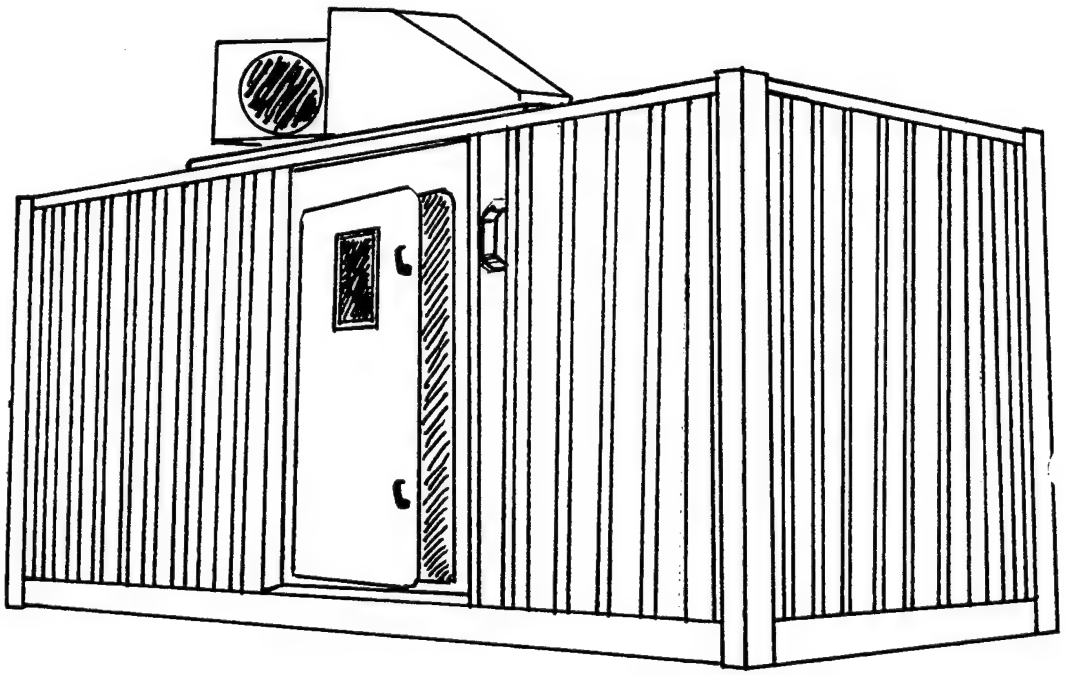

Figure 5. Volume imaging lidar shelter.

Electrical Modifications

A 200 amp breaker panel was installed on the interior, rear-wall of the shelter. Three-phase, 240V, 100A power and 60A, 208V, single phase power is available to the laser. There are disconnect switches installed inside the shelter to remove power from the laser and the scissor

jack. The disconnect switches for the heat exchanger and water pump are located on the exterior, rear wall just above the units they control. There are several single phase, 115V, 20A branch circuits used for lighting and outlets. The outlets are distributed throughout the shelter with several located directly behind the equipment racks. Appendix 3 contains drawings showing exact locations of wiring, disconnects, outlets and other information regarding modifications made to the shelter.

Heating and Air conditioning

Air conditioning, heating and ductwork were added to keep the interior temperature of the shelter stabilized for the proper operation of lasers, computers and sensors. The rear of the shelter was sectioned off from the main operations area to make room for the air conditioner and heat exchanger. The heat exchanger was added to cool the hot water exhausted from the laser and power supply. A pump is positioned in the rear section of the shelter to pressurize the cooling water. Standard garden hose is used to connect the heat exchanger and pump to spigots mounted on the exterior rear wall of the trailer. Copper pipes, installed within the walls of the shelter, allow the cooling water to flow to the laser system.

Modifications Made to the Shelter Roof

The roof of the shelter has a 4′ by 6′ rectangular hole cut in it, the edges of which are raised to prevent water from entering the shelter. During lidar operations, the scanning mechanism is raised through this hole by a hydraulic scissor-jack that is bolted to the floor. When the lidar is inactive, a lightweight, aluminum cover is placed over the hole in the roof and clamped in place.

Access to the roof can be gained by two methods. A ladder mounted on the rear of the shelter provides the easiest access but fold down grips attached to the front face of the shelter can be used when necessary. For safety, a railing has been installed along one side of the shelter roof.

Phone Lines

Phone lines were added to the equipment shelter for voice and data communications. Modular RJ11 phone jacks were placed on the wall near the VIL operator's control-area and also behind the equipment racks for computer access. The phone line is brought in through the access panel located near the roof line of the shelter.

Access Panel

The access panel is used to bring wiring in and out of the lidar trailer through watertight connectors. GPS antennae, magnetic compass inputs, an external kill-switch, telephone lines, and 120 VAC power, are available at the panel. Listed in Appendix 4 are the connector types, their functions and pin-outs.

Laser Interlock

An interlock system, installed throughout the shelter, is used to turn off the laser in an emergency. The laser system is supplied with circuitry that checks for continuity between two points. Depending on the laser manufacturer there may be either a very low current (0.1A) 110VAC signal or a 5 to 15 VDC signal used to detect an open circuit. If an open circuit is detected, the laser automatically shuts down. In our system, this port is connected into an interlock network that runs throughout the shelter as well as outside to an external kill-switch. Quick disconnects and switches are provided at the points shown in appendix 3.

Within the shelter there are several locations where you can interrupt laser operations:

1. Laser KILL switch located on front of rack above computer.
2. Quick disconnect located on wall behind VIL operator.
3. Magnetic KILL switch mounted on access door.
4. Quick disconnect on wall near laser bench.

Operation of the lidar requires an observer and an operator. The observer is located outside the shelter. He scans the zone in which the laser is being operated and looks for any potentially hazardous situations. The observer has a kill switch that is wired directly into the exterior, interlock-connector through the access panel. If any unsafe situations arise, the laser is immediately shut down.

Radar Safety

A Raytheon Model R72 Raster Scan Radar is another safety feature the VIL uses. The radar monitors boat and air traffic in the vicinity of the VIL. The radar can detect traffic at ranges up to 72 nm. The system consists of a scanning unit and display unit. The scanner housing contains a 10 Kw transmitter, a low-noise front-end, the antenna drive motor and control circuitry. A single multi-conductor cable attaches the scanner to the display unit.

The display unit can be programmed to generate a warning tone when a ship or plane enters a predetermined sector. This sector can be adjusted by selecting upper and lower azimuth limits and a range limit with respect to the VIL site. This forms a pie-shaped segment that ship and aircraft can not enter without triggering an alarm. A radar-warning-detector was built and wired into the VIL interlock system. If the radar warning tone sounds, the laser is automatically shut-down.

5. Volume Imaging Lidar Components

The VIL is made up of several components including a laser, a scanning system , a receiving telescope, and a photodiode sensor package. These components are mounted on a rigid frame that can be raised and lowered within the weather-proofed VIL shelter described above. Following is a discussion of each of the components and their uses.

Lidar Mounting Frame

The lidar components are mounted on a welded, aluminum frame approximately 6′ in length, 4′ wide and 5′ tall. The frame was designed for maximum rigidity since any flexure of the optical components or mounting rods would cause the VIL optics to move out of alignment. This frame is designed to hold the laser, scanning mirrors, receiving optics and sensor as well as vertical and directional gyros during shipboard use of the system.

The frame is bolted to a hydraulic, scissors-jack manufactured by Presto. The jack, a model XL-T48L20, has a lifting capacity of 2000 pounds and is used to raise the scanning mechanism through the opening in the shelter roof during operations. In this way, the scanning mechanism can be stored inside the trailer to protect the mirrors and scanning system from the effects of the weather when it is not in use.

The lidar frame is positioned within four, steel guide-rails mounted at each corner in which the frame can slide vertically. These rails are bolted to the floor and the ceiling of the shelter. Their purpose is to constrain the lidar frame during hydraulic scissor-jack use. When the system is raised above the roof line of the shelter, the lidar frame is pinned to the guide rails and the scissor jack is blocked in position so the weight of the lidar frame is supported by pins and blocks rather than the scissor jack. Air filled shock absorbers are mounted on the base of the frame to reduce impact to the equipment when the lidar frame is lowered and to minimize vibration when the shelter is moved.

The frame has a 0.25″ thick, aluminum deck. A rubber gasket extends beyond the outer edge and overlaps the cutout in the roof by several inches to obstruct rain that would otherwise enter the shelter. The deck has a slight curvature to force rain-water to run off rather than collect and puddle.

The scanning mechanism is positioned directly over a 20″ diameter hole cut in the lidar frame deck. This is where the laser beam exits the shelter and scattered return-light enters.

Laser

The VIL is designed to be operated with either a Continuum 50mj Nd:Yag operating at 500 Hz or a Spectra Physics 750 mj Nd:Yag operating at 10 Hz used during aircraft operations. Both lasers operate in the near infrared at a wavelength of 1064 ηm, which is invisible to the human eye. They are both class IV lasers and can represent a serious eye hazard if not operated correctly. Normally, the laser beam is enclosed behind a sheet metal cover, protecting the operator from the beam. However, if the covers are removed then goggles must be worn. Beam parameters of both lasers are given in table 1.

The laser's principle function is to provide a backscatter source for aerosols in the sensing volume. Important considerations for laser choice include the pulse width, divergence, cross-sectional beam shape, power output levels and stability, as well as repetition rate.

Parameter	Continuum	Spectra Physics
Wavelength	1064 nm	1064 nm
Pulse Duration	8-12 ns	8-12 ns
Power Output	25 mj	500 mj
Pulse Repetition	540 Hz	10 Hz
Average Power	14 w	5 w
Beam Divergence	2.0 mrad	1.0 mrad
Beam Diameter	3.5 mm	7.0 mm
Energy Stability	$\pm$7.0%	$\pm$1.0%

Table 1. Beam characteristics of the NRL VIL system lasers.

Both lasers require external power and cooling. The Continuum laser uses 240 VAC, 100A, 3ϕ power and requires cooling water at a flow rate of 3 gal/min at a maximum temperature of 25 $^{\circ}$C. The Spectra Physics laser requires 208 VAC, 50A, 1ϕ power and cooling water at a maximum temperature of 25 $^{\circ}$C and a flow rate of 1 gal/min.

Each of the lasers has a continuity check point built into the laser power supply that is wired into the VIL system interlock. The Continuum laser places a 15 VDC, low-amperage signal on the interlock system. The Spectra Physics laser places 110 VAC at about 0.1A on the interlock system. Although the variation of voltage does not affect interlock operation, care should be taken not to become part of the electrical path in the case of the 110 VAC source, a mild shock could be felt at 0.1A.

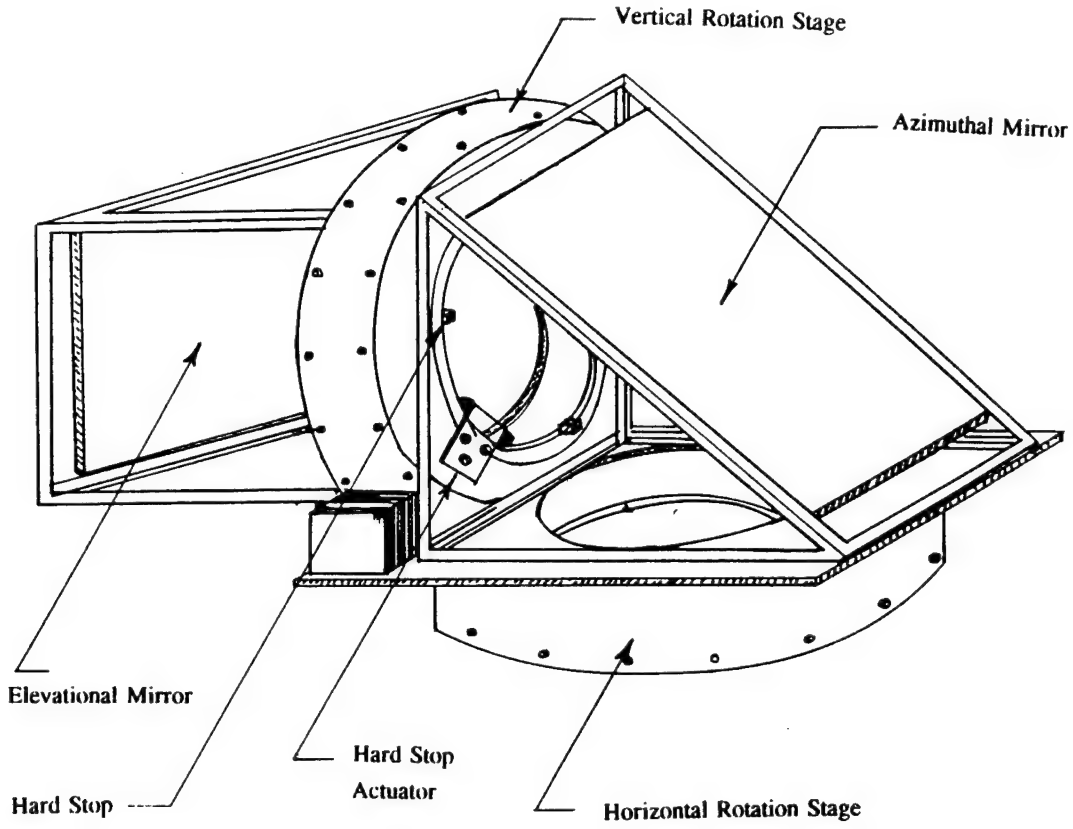

Figure 6. Description of the VIL scanning mechanism.

Scanning System

The scanning mechanism, depicted in figure 6, directs the laser beam into the atmosphere and directs the return light into the receiving telescope. It consists of two Klinger RT660 rotation stages and two, large, coated mirrors. The rotation stages each have a 19" diameter hole in their center as shown in figure 7. The outer ring of the horizontal rotation stage is fixed to the lidar frame. The inner ring is free to rotate continuously in either direction. The outer ring of the vertical rotation stage is rigidly attached to a plate that turns with the horizontal rotation stage. Both stages are positioned by stepper motors that are controlled by a 486 PC and a stepper controller located in the lidar shelter. A helical gear is located on the side of the rotation stages and stepper motors are attached at this point.

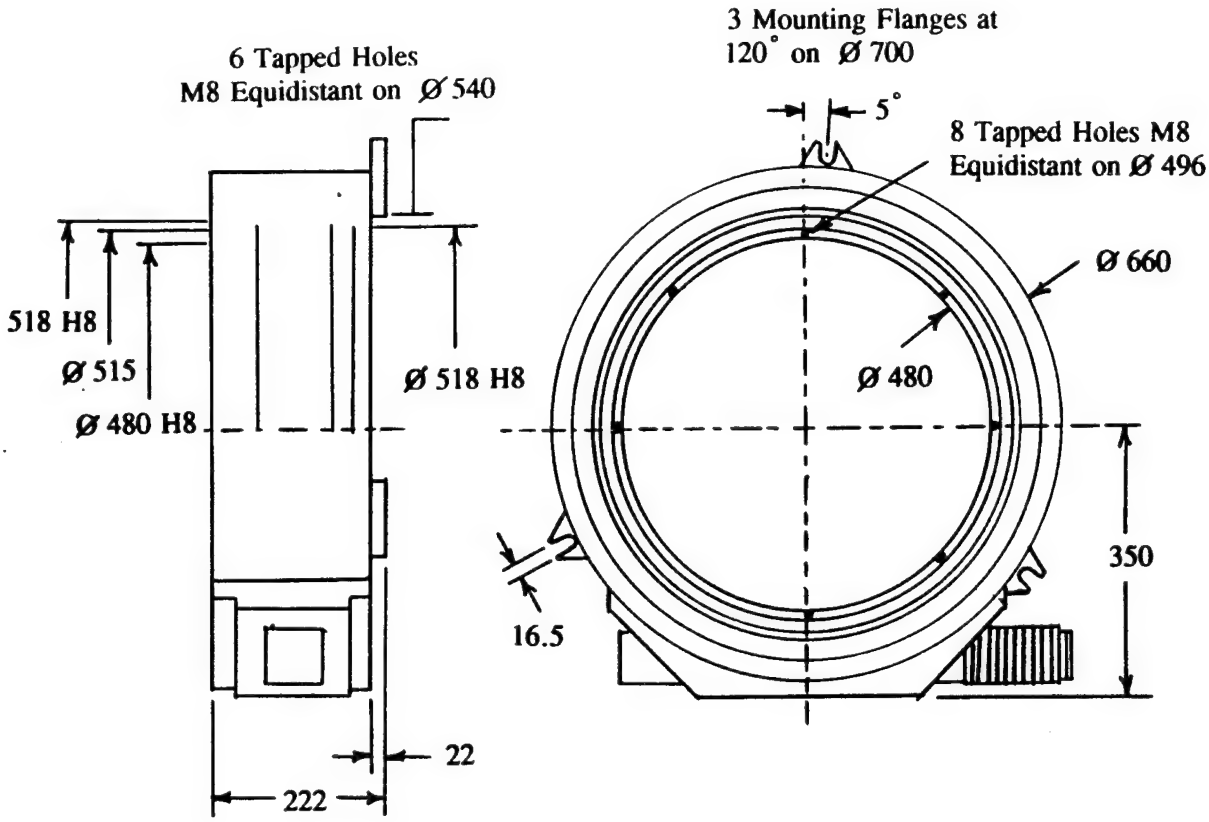

Figure 7. RT660 rotation stage.

The scanning mechanism can scan in azimuth and elevation at angular velocities ranging from $0.01^{\circ}s^{-1}$ to as high as $40^{\circ}s^{-1}$ .The stepper motor can change position of the rotation stages in increments of 0.001° with a precision of 0.001°. The stepper-motor controllers are attached by cable to each rotation stage. The controller provides the ability to change the position, velocity and acceleration of the scanning mechanism and also provides information about the present location and velocity.

The rotation stages are mounted perpendicular to each other with the mirrors mounted to the stages at 45° to the plane of rotation, see figure 6. The reflective-surface of the mirrors face the 20" diameter openings in the rotation stages. The horizontal stage is bolted above the 20" diameter hole in the deck plate of the lidar frame, see figure 8. The laser is aimed directly up through this hole and reflects off the two mirrors and into the atmosphere. The return signal is scattered back toward the mirrors and reflects off the mirrors down into the shelter where it is focused by the receiving telescope onto a photodiode.

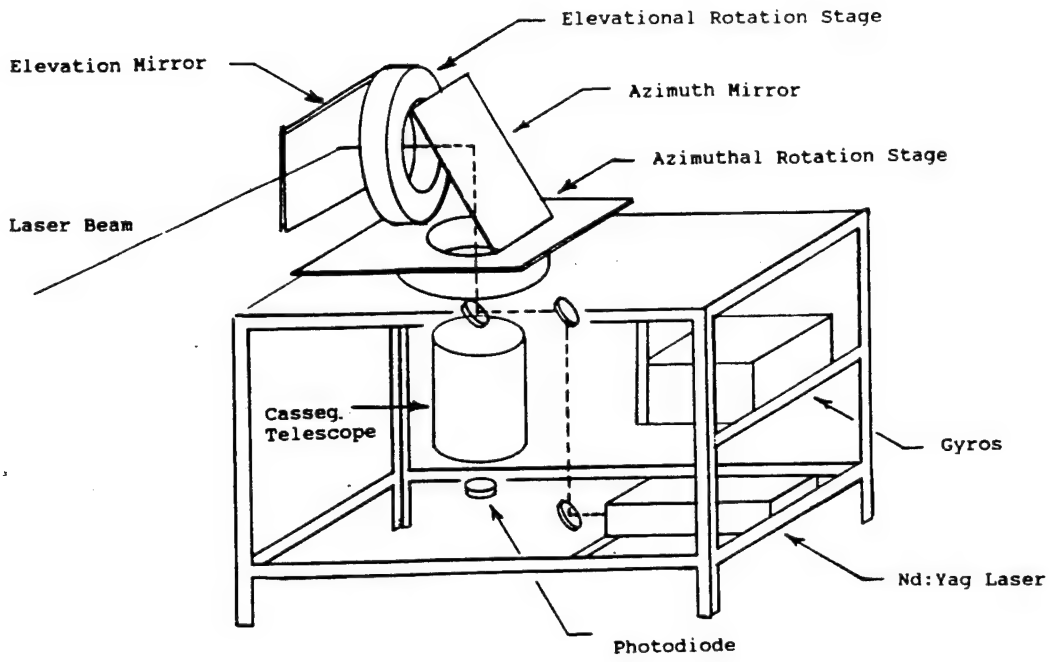

Figure 8. Scanning system layout.

The horizontal stage rotates both mirrors and controls the azimuthal pointing direction. The vertical stage rotates the second mirror and controls the elevation. The scanner can be rotated in azimuth approximately $\pm 270^{\circ}$ and is limited to this because of cables that run through the center of the rotation stage. The elevational scanner can rotate continuously 360°. There are two reasons that the scanner movement must be limited. First, and most important, the scanner controls the pointing direction of the laser beam, its movement must be limited for safety. Second, the azimuthal rotation stage has cables that run through its center so rotations must be limited or the cables would be damaged.

Two methods are used to ensure that the scanner operates within its prescribed boundaries. The system software sets "soft limits" both in azimuth and elevation that limit the movement of the scanner to a predetermined area. The controller will not perform a move outside of these angular limits. As a secondary precaution, hard-stops, pictured in figure 6, are used to ensure that the scanner can not move beyond the desired limits. The "soft limits" are a few degrees inside of the hard-stop locations. The hard-stops are used only as a last resort.

The hard-stops consist of 0.75″ square aluminum rods approximately 2″ long. They are bolted to the rotation stage and move with the azimuth and elevational stages. The hard stop actuator is bolted to a part of the rotation stage that does not move. It has arms that protrude down into the path of the hard stops. Rubber bumpers are attached to these arms to reduce damage to the stops, rotation stages and mirrors if the "soft limits" fail.

Scanning Electronics

The scanner positioning is controlled by the 486 PC that sends commands to the stepper controller. The stepper controller, the Motion Master 2000 (MM2000), Model Step 1.5M, is installed inside the 486 PC and converts the commands generated by the lidar system software to signals that the stepper motor can use.

Transmission Optics

The laser transmission path is shown in figure 9. The laser beam reflects off the first mirror (M1) mounted at 45° to the beam, travels through a power meter (PM1), reflects off the second mirror (M2) that redirects the beam onto the third mirror (M3) mounted coaxially with the receiving telescope. The laser beam is redirected by M3 out of the shelter and onto the first large scanning mirror (M4). The beam is reflected by M4 onto the elevational scanning mirror (M5) into the atmosphere. Table 2 lists the mirrors, by the numbers listed in figure 10, and their specifications.

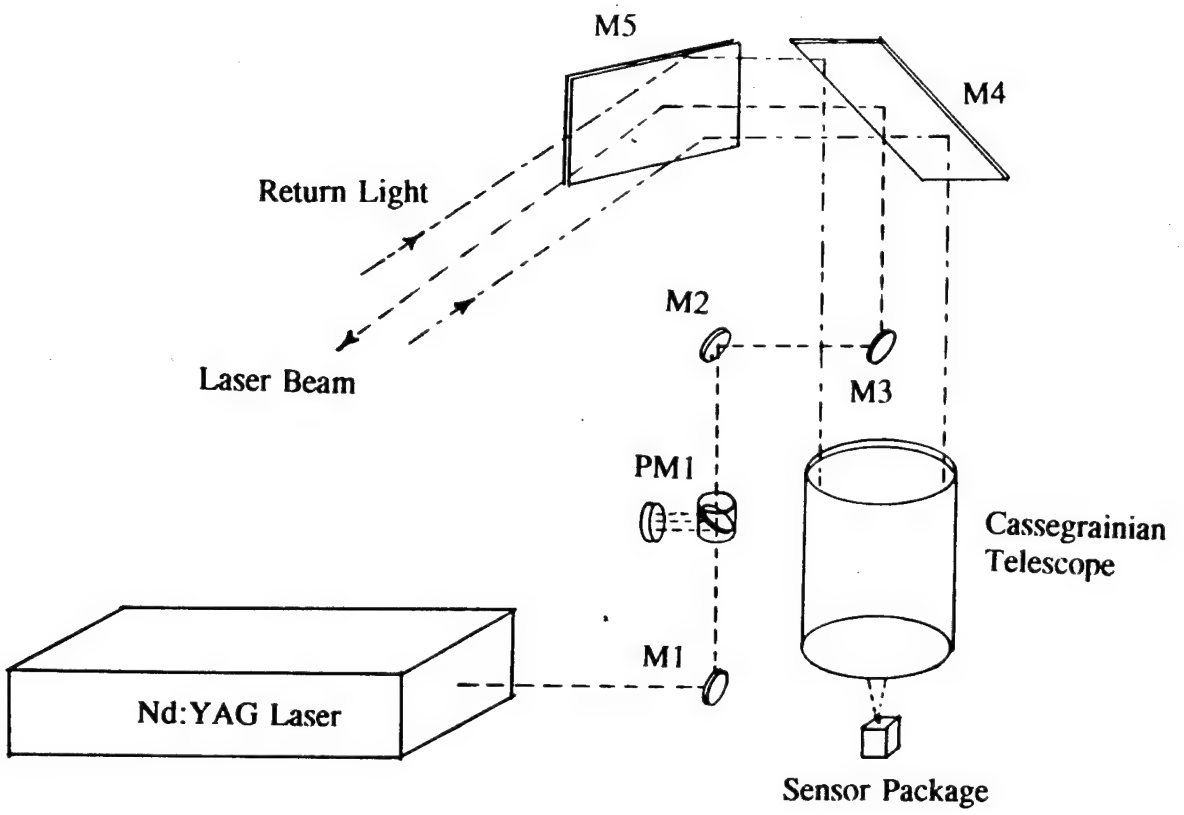

Figure 9. Laser beam transmission path.

Mirror	Size	Thickness	Smoothness	%Trans/Coating/
M1	4.0"	1.0"	λ/50	98% /IF/1064 nm
M2	4.0"	1.0"	λ/50	98% /IF/1064 nm
M3	2.5"	0.5"	λ/50	98% /IF/1064 nm
M4	19"x24"	1.0"	λ/5	60% /IF/1064 nm
M5	19"x24"	1.0"	λ/5	60% /IF/1064 nm

IF = Interference Film

Table 2. Transmission optics specifications.

The scanner mirrors are made by NU-TEK Inc. They are rigidly attached to the rotation stages. There are slotted mounts that allow a slight adjustment of the mirrors for alignment purposes. The mirrors are coated to reflect light only at 1064 ηm. This is because first, the lasers are powerful enough that they could burn a silvered, multi-wavelength coating and ruin the surface and second, by restricting the wavelengths of light that can be reflected into the telescope, the signal to noise ratio is significantly improved, especially during daylight operations.

The three, smaller mirrors, M1, M2, M3 are made by Melles-Griot. They are attached to adjustable, optical mounts. The mounts have been modified to allow the mirrors the adjustability necessary to align the system. See appendix 3 for further information on system alignment.

Receiving Optics

The two large scanning mirrors, M4 and M5 described above, are the first components in the receiver path. Light, elastically scattered in the atmosphere, is reflected back onto M5 in figure 9. M5 redirects the light onto M4 which in turn reflects the light onto the collecting mirror of a Cassegrainian telescope.

The Cassegrainian telescope used in this system is a Celestron Inc. Model C 14. Figure 10 shows a schematic diagram of this type of telescope. Its primary mirror has a clear aperture of 14".

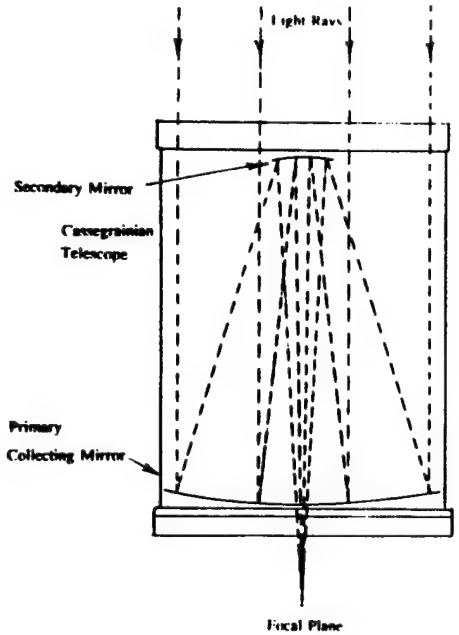

Figure 10. Cassegrainian telescope operation.

The telescope sits directly beneath the horizontal rotation stage and focuses the return light onto a silicon, avalanche photodiode sensor. The telescope has adjustment capabilities for moving the focus and for recollimating the telescope. The telescope is rigidly mounted to the lidar frame above the sensor.

Sensor Package

There are two sensor packages used in the VIL system. The type used most often is a silicon avalanche photodiode(APD) with a built in log amp made by Analog Modules, Inc. It is mounted directly under the receiving telescope on translation stages capable of adjusting the sensor position in a 25 cm^2 area. The sensor height can also be adjusted to bring the sensor into the focal plane of the telescope.

The sensor package contains a logarithmic amplifier to extend the range of signal strengths the system can measure. The sensor package uses a C30956E APD as a detector. It has a responsivity of 25 A/w at 1060 ηm, a dark current of 174 ηA, and a noise current of 2.1 $pA/Hz^{1/2}$.

A photomultiplier tube, model R632-01, can be used as the backscatter sensor and is used as an aureole sensor in aircraft operations. It is manufactured by Hamamatsu Corporation and has a luminous sensitivity of 64.3 A/lm and a dark current of 650 ηA.

6. Data Acquisition Hardware

The data acquisition system is comprised of a 486 PC which functions as the system controller (see appendix 5 for DMA and interrupt information), a CAMAC data acquisition unit that provides signal conditioning, a power meter for monitoring laser output energy and a Silicon Graphics workstation used to display the data and provide data-storage.

As shown in figure 11, the 486 PC performs several tasks that include:

1. Controlling the scanning mechanism and providing user interface for adjustment of scanning parameters.
2. Initializing and controlling the CAMAC data acquisition modules.
3. Reading data from the CAMAC interface.
4. Reading data from the laser power-meter.
5. Combining header information, CAMAC data, and power meter data into a single structure.
6. Sending the data structure to the SGI for storage and display.

The SGI workstation, an Iris Indigo Elan, is used to create realtime 2-D and 3-D displays of aerosol structures, calculate winds and turbulence, and serve as the data storage device. A

1.2 Gb SCSI Python DAT drive manufactured by Archive is mounted in the SGI and provides fast, reliable, and inexpensive data storage. The DAT drive can store data continuously at nearly 1 Mb/s.

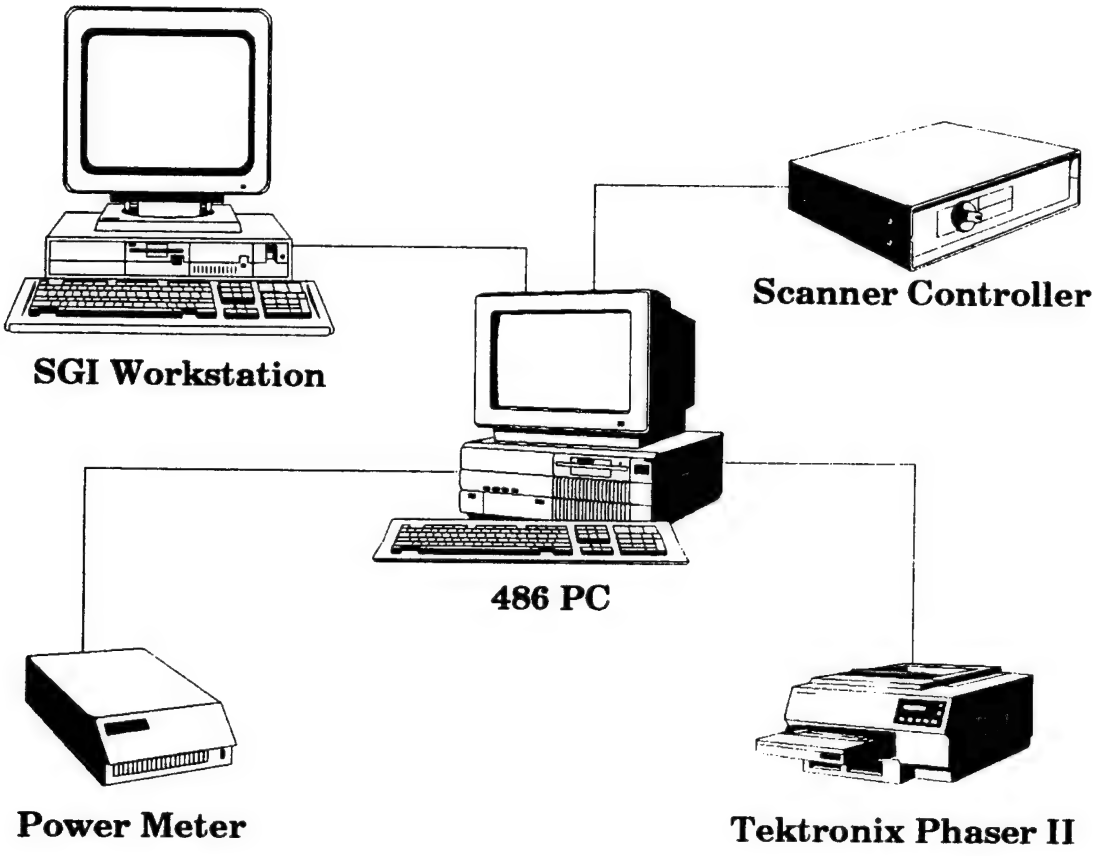

Figure 11. VIL computer interconnections.

CAMAC Data Acquisition Unit

The CAMAC Crate (IEEE-583) is a modular, realtime interface for high performance data acquisition systems. The crate itself is a rack mountable enclosure that can hold several CAMAC modules. The modules perform functions such as signal digitization, averaging, and amplification. The VIL uses the following CAMAC modules:

1. TRANSIAC 2010S - 20 MHz, 10 bit Transient Recorder
2. TRANSIAC 4100 - Signal Averager
3. TRANSIAC 1020 - Differential Amplifier
4. KSC 3929 - SCSI Controller/Interface
5. DSP 2001 - 100MHz, 12 bit Transient Recorder
6. DSP 4101 - Signal Averager
7. LeCroy 6102 - Amplifier

In the basic, ground-based VIL system, the TRANSIAC 2010S, TRANSIAC 4100, TRANSIAC 1020 and the KSC 3929 SCSI Controller are used. The other modules are used to acquire the aureole signal during airborne use of the VIL system. In figure 12, the CAMAC module interconnections are shown. The sync pulse from the variable laser sync-output provides system timing. A list of CAMAC manuals can be found in appendix 6. For further information regarding the operation of the CAMAC modules please refer to their respective manuals.

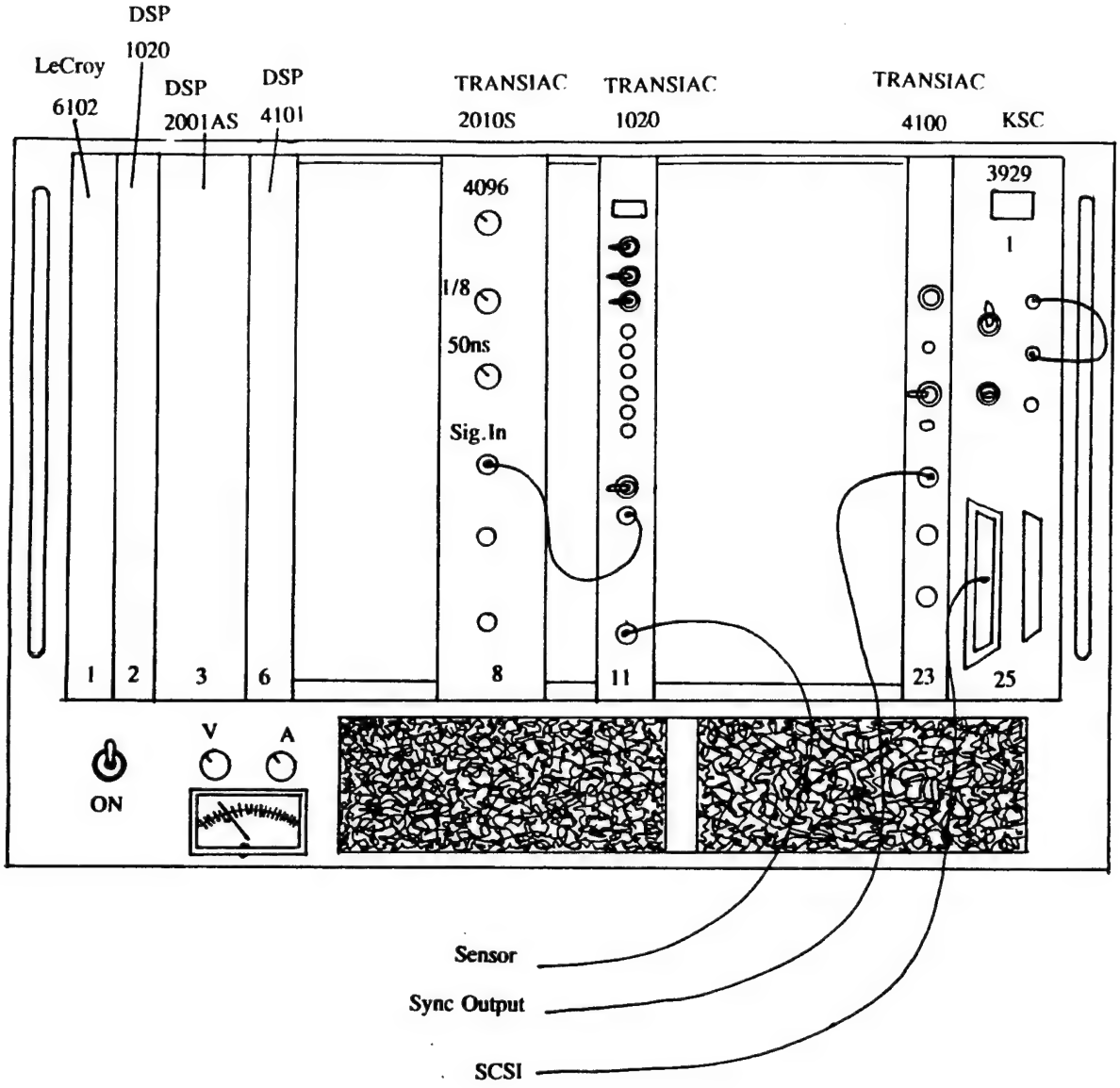

Figure 12. CAMAC module interconnections.

Data Storage and Display

A Silicon Graphics Inc. IRIS Indigo Elan workstation is used as the display and data storage device in the VIL system. It runs IRIX, a modified, SGI version of UNIX, as its operating system. SGI workstations are specially designed for high speed graphics. The display, a 20" monitor with 24 bit color and Z-plane buffering, has specially-designed, graphics accelerators built into hardware that speed graphics rendering.

An external SCSI port is used to attach the SGI to the 486 PC and a Tektronix Phaser II color printer. An internal DDS digital audio tape (DAT) drive is mounted in the SGI. The DAT drive can store 1.2Gb of data on a single DAT tape. The tapes used in the VIL are Maxell Heli Scan DDS 4mm DAT tapes, 60 m in length. The maximum data rate for the SCSI bus is approximately 5Mb/s but the DAT tape limits transfers to about 1Mb/s. Data storage costs are about $8.00/Gb.

7. Data Acquisition Software

The data acquisition software consists of two sets of software; one set runs on the 486 PC and the other set runs on the SGI system. The 486 PC acts as the system controller. The flow chart shown figure 13 shows the order of events that take place during the data acquisition cycle. The 486 PC is the system controller as described above, and is responsible for moving the scanner, initiating CAMAC operations, reading the CAMAC data, and sending data to the SGI for display and storage.

The data record is stored as a structure of 512 bytes of header information that includes date and time, azimuth, elevation, laser power, etc. and a 16Kb block of lidar data. Generally, the data block has 4096 range points with 4 bytes of information per point. The data block-length is adjustable depending on the range required. Appendix 7 lists the header information and storage format in more detail.

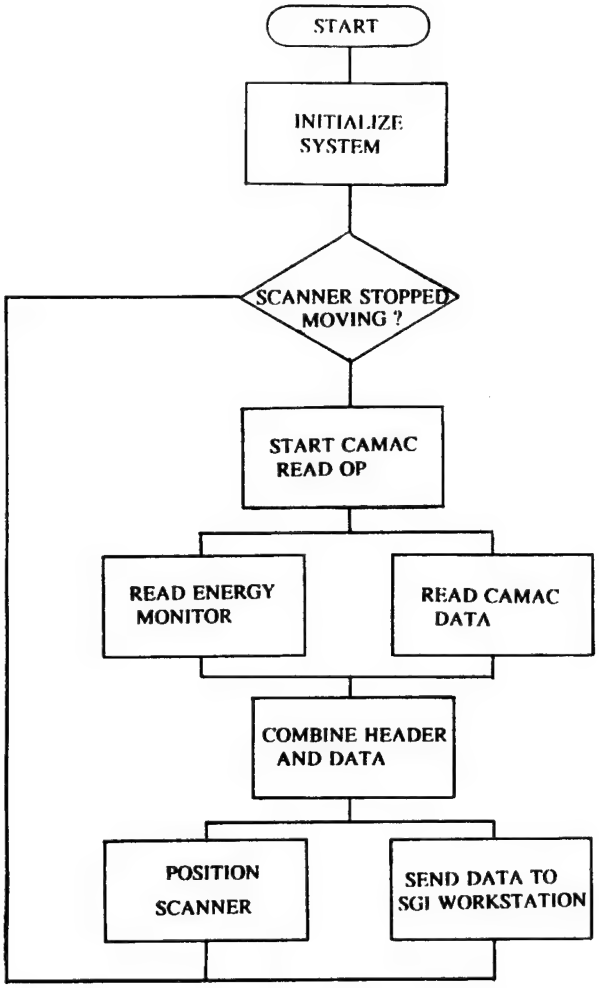

Figure 13. Order of events during the data acquisition cycle.

The VIL system software is comprised of many libraries and include files. More detailed descriptions of each of the programs and associated files can be found in Appendix 8.

8. Lidar Capabilities

The VIL is capable of making a wide-assortment of measurements for many purposes. It can provide a means to visualize the dynamics of the atmosphere and its characteristics. The capabilities described below are just a few of the many possible uses of the VIL.

3-D Analysis of Aerosol Structures in Realtime

The volume imaging lidar provides researchers with a tool for viewing aerosol structures, both visible and sub-visible, as 3-D volume images. This analysis can be done in realtime allowing true 3-D visualization of atmospheric processes.

The lidar is scanned in a repetitive fashion by changing the azimuth and elevation of the scanning mechanism. The return signal is analyzed and displayed on an SGI color monitor. Many views are available for study including 3-D images of aerosol structures, vertical cross-sections, constant-range cross-sections, horizontal cross-sections and more. Aerosol structures can be dissected and studied and their movement analyzed in realtime. For example, from a series of volume scans, data can be sorted according to varying elevation angles and by looking at all return values at constant elevations, a slice of the atmosphere can be studied. Increasing the elevation angle allows the study of aerosol structures one slice at a time. The 3-D capabilities of the NRL VIL are graphically depicted in figure 14 which shows a volume scan of the Tilghman Island tower.

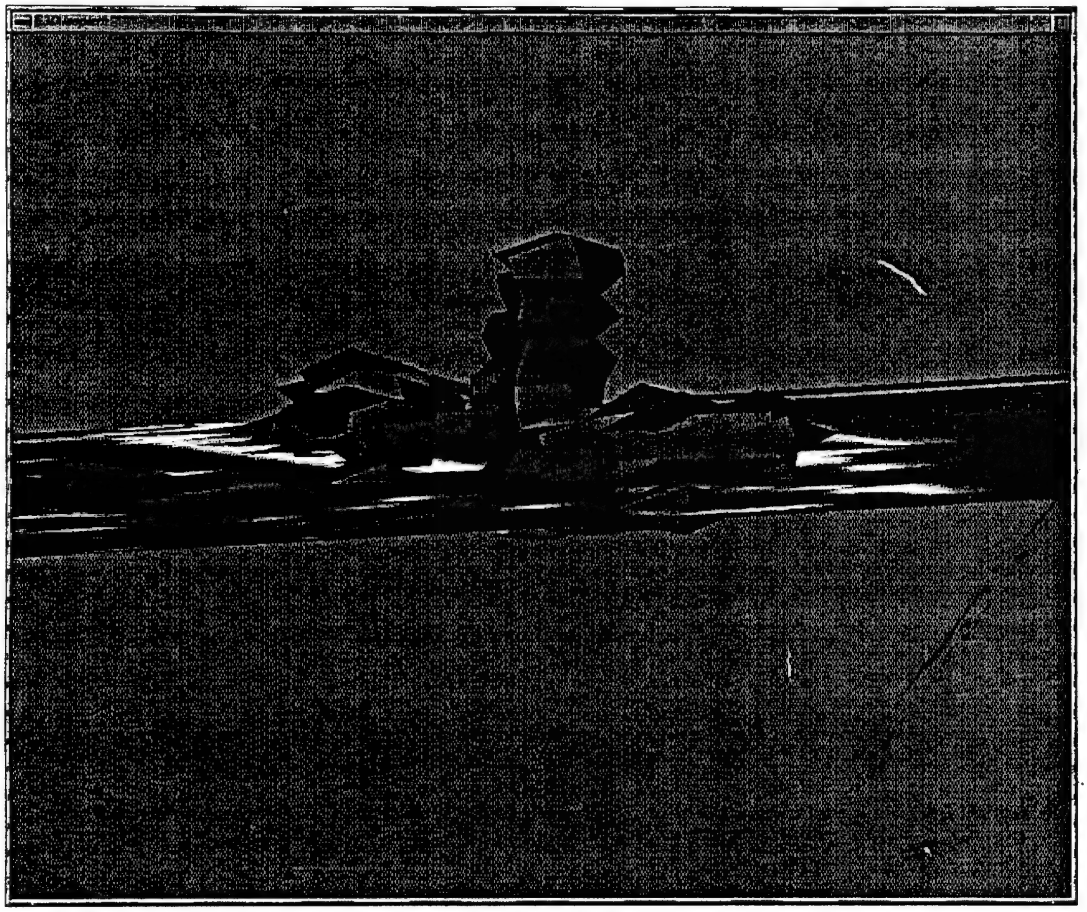

Figure 14. 3-D image of the NRL tower on Tilghman Island.

Analysis of Optical Properties

The lidar can provide an insight into the electro-optical (EO) characteristics of the atmosphere such as EO wave propagation. By operating the lidar from aircraft, estimates of the extinction coefficient can be made. By using both the backscatter profile and the surface return, which provides information on the extinction-backscatter relationship[4], extinction can be calculated from the inverted backscatter signal. Please read the section entitled "Airborne Use of the Lidar Equipment" for further information.

Ship Tracking

The NRL VIL participated in the Monterey Area Ship Track (MAST) experiment[5] held off the coast of the western United States in the summer of 1994. The purpose of MAST was to study ship-tracks that have been photographed by satellites, over cloud-covered portions of the ocean, for many years. These satellite images contain long, linear features, sometimes hundreds of miles long, that are significantly brighter than the surrounding clouds. The tracks have been traced to ship movement but their causes are not fully understood. Scientists from several nations joined to determine the conditions under which these ship-tracks form.

The lidar was modified for shipboard use and mounted to the deck of the RV GLORITA, see figure 15. Beam pointing stabilization was accomplished using gyros to measure the pitch and roll of the ship[6].

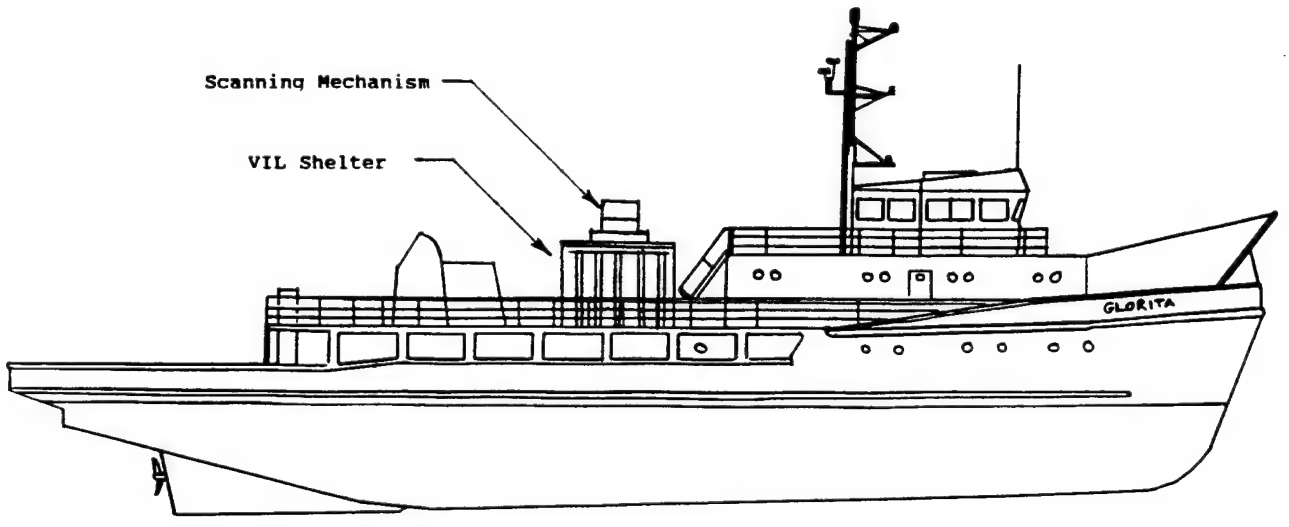

Figure 15. Shipboard configuration of the VIL.

Ship tracks from many ships were detected by the VIL, both those from Navy ships participating in the experiment as well as ships that traversed through the measurement area. A ship track measured behind an unidentified commercial freighter is shown in figure 3.

Realtime Analysis of Cloud Formation

During the Big Sur extension[7] of the MAST experiment which was held in July of 1994, the VIL was positioned about a half mile downwind of a large (approximately 500m at the base and 120m tall), rock mound at Big Sur, Ca. The predominant wind during the experimental period was caused by a low level wind maximum and consistently blew at approximately 40 mph from the Northwest.

The presence of the rock in the wind field caused lifting of the air parcels and subsequently, clouds formed at the apex. The clouds grew for a short period of time and then slowly decayed as they drifted downwind of the rock. The lidar was in a position to make volume-images of the atmosphere both before and after the rock. Figure 16 shows a horizontal cross section of the area with the influence of the rock clearly visible. Information of this type can be of extreme importance to climate modelers. The effects of coastal topography can have major effects on local climatology.

In future experiments of this type, the scanning of the lidar could be dynamically controlled. After the wind speed and direction is measured, the lidar would scan a volume in a repetitive pattern and the scanning volume gradually moved with the wind allowing the evolution of the aerosol feature to be observed. Volume-images could then be made of the cloud as it grew and decayed. Statistical analyses could be made of cloud formation and decay.

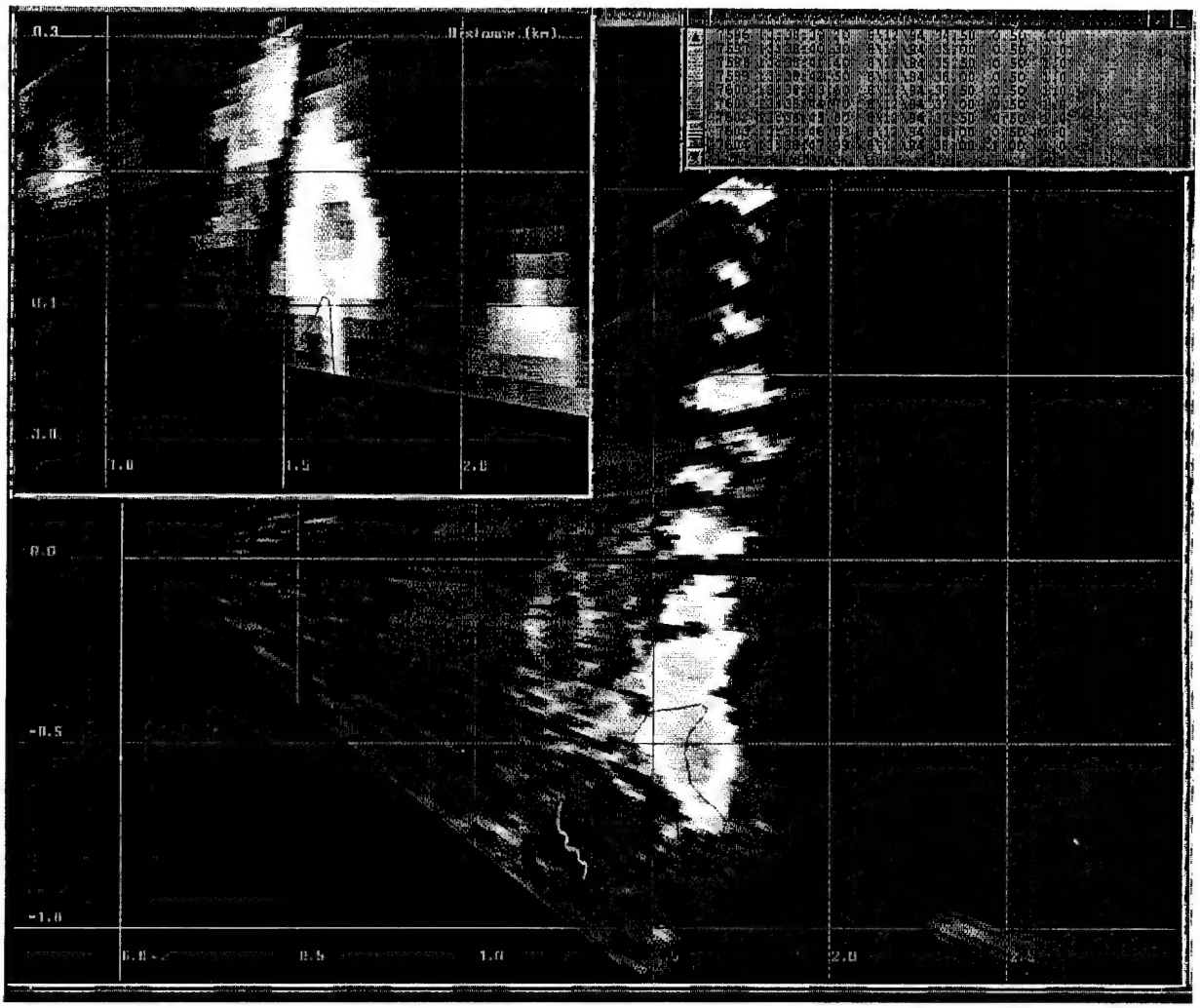

Figure 16. PPI scan of the rock showing its effects on aerosol structures.

Realtime Wind Speed, Direction and Turbulence

The measurement of accurate wind velocity and turbulence is not an easy task because structures such as oil platforms, boats, aircraft, and towers, which are typically used to mount wind measurement systems, dramatically influence the wind field. Because of this, anemometers are typically very inaccurate[8]. The lidar can measure wind fields over a wide area in realtime without influencing the measurements.

Wind speed and turbulence measurements can be made by a scanning lidar by analyzing the coherence of spatially and temporally-separated lidar returns[9]. A multi-angle scan is performed and the returns are analyzed statistically in Fourier space. This method provides information on wind speed, direction and turbulence in the atmosphere.

During the Pt. Sur experiment, TAAS (triple azimuth angle scans) were made. Figure 17 shows a grey scale image of a TAAS as well as the coherence curves associated with this scan.

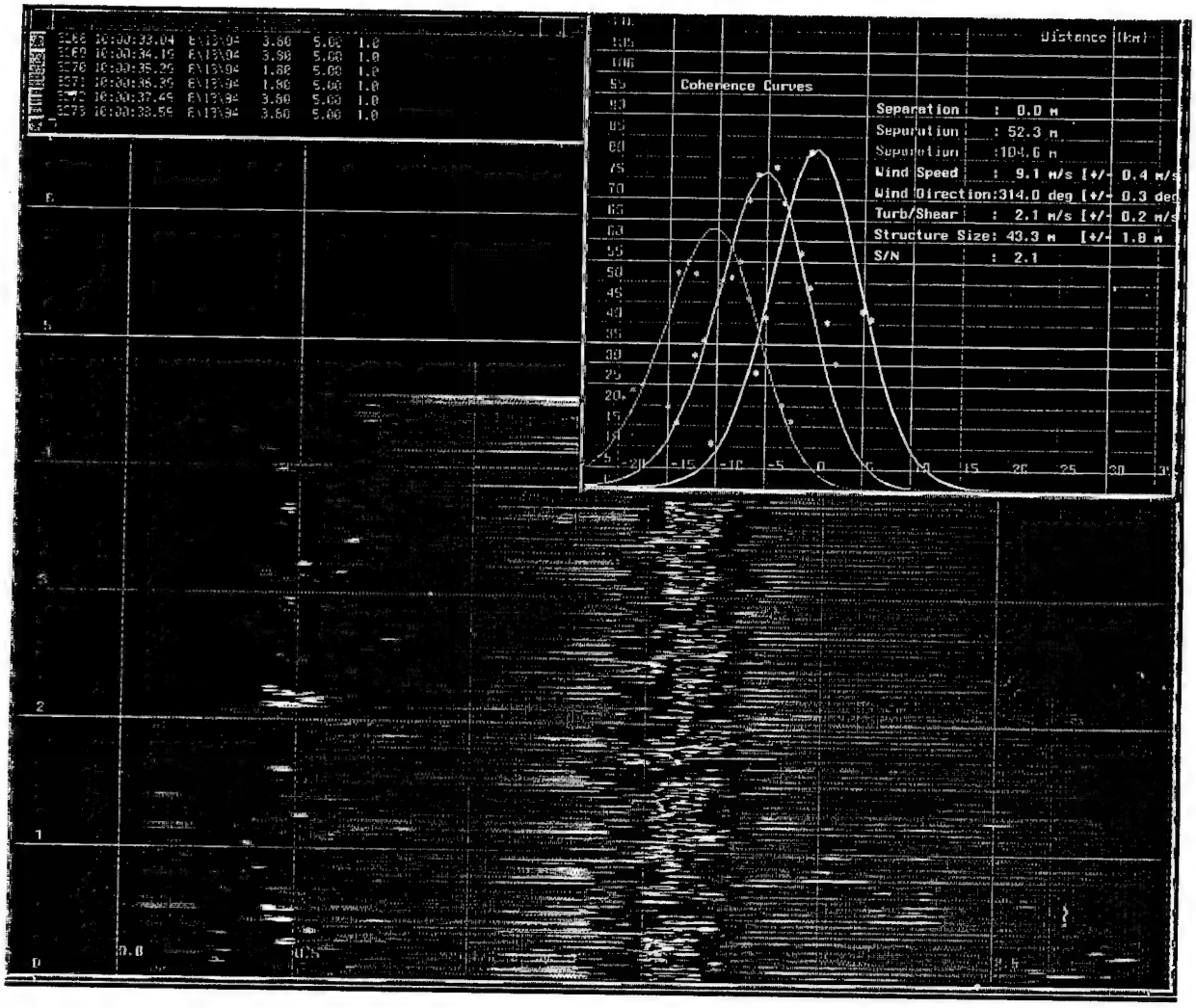

Figure 17. Image of coherence curves and wind speed from TAAS. Note the wind measurements can be made in real time.

Boundary Layer Measurements

The marine boundary layer (MBL) or inversion layer is the height in the atmosphere where there is a large gradient in the temperature and humidity profiles. This layer effects radiative cooling rates, upper and lower atmospheric mixing, EO wave propagation, and many other atmospheric processes.

The lidar can measure the boundary layer-height and depth from both ground-based and airborne, down-looking lidar. The MBL, as portrayed by a lidar false-color image, is pictured in figure 18. The data was taken over the Pacific ocean during VOCAR experiment in 1992.

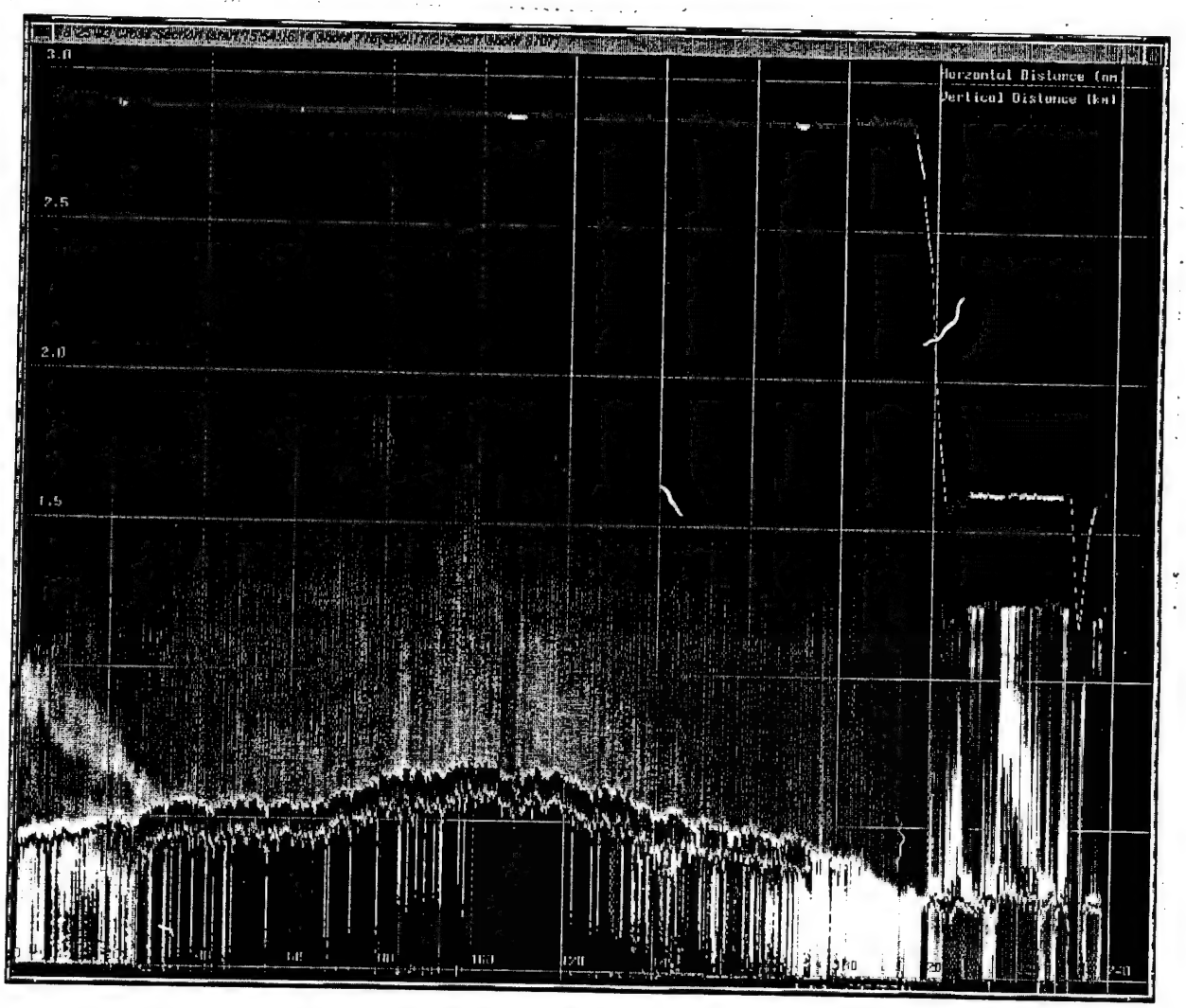

Figure 18. Marine boundary layer scanned by the airborne lidar.

9. Shipboard Use of the VIL

The VIL is capable of making scanning lidar measurements aboard ship which makes remote, ocean-sites (whose atmosphere is unaffected by land masses) accessible.

During the MAST experiment, the VIL was operated aboard ship to detect and create 3-D volume-images of ship-generated plumes. The system operated throughout the entire cruise without failure. VIL measurements were even made during periods of heavy-surf, although re-alignment of the optics was necessary.

Several problems arise when faced with making scanning lidar measurements aboard ship. The movements of a ship's deck can produce substantial pointing errors for a scanning lidar. For example, a 5 degree roll creates a positioning error of nearly 175m vertical displacement from the desired position at a range of 2km. To use the lidar aboard ship it is necessary to correct for this motion. Modifications must be made to the VIL hardware and software to operate aboard ship.

Hardware Modifications

Hardware modifications to the VIL system include the addition of vertical and directional gyros, an 8-channel differential A/D board and a second 486 PC. The gyros, made by Humphries, Inc. are used to measure the pitch, roll and yaw of the ship.

The A/D board, a Data Translation DT2801/5716, digitizes the analog gyro-outputs. It has 16-bit resolution and a maximum sampling rate of 5 Khz. The DT2801/5716 is sampled at about 10 Hz in the VIL configuration.

The 486 PC, labelled "Scanner PC" in figure 19, is used to continually interrogate the gyro outputs via the DT2801 and compute position corrections. The SGI operates the same as it does in the ground based VIL. The 486 PC labelled "Lidar PC" operates the same as in the ground based system except that rather than sending scan angles to the scanning mechanism directly, the angles are sent to the "Scanner PC".

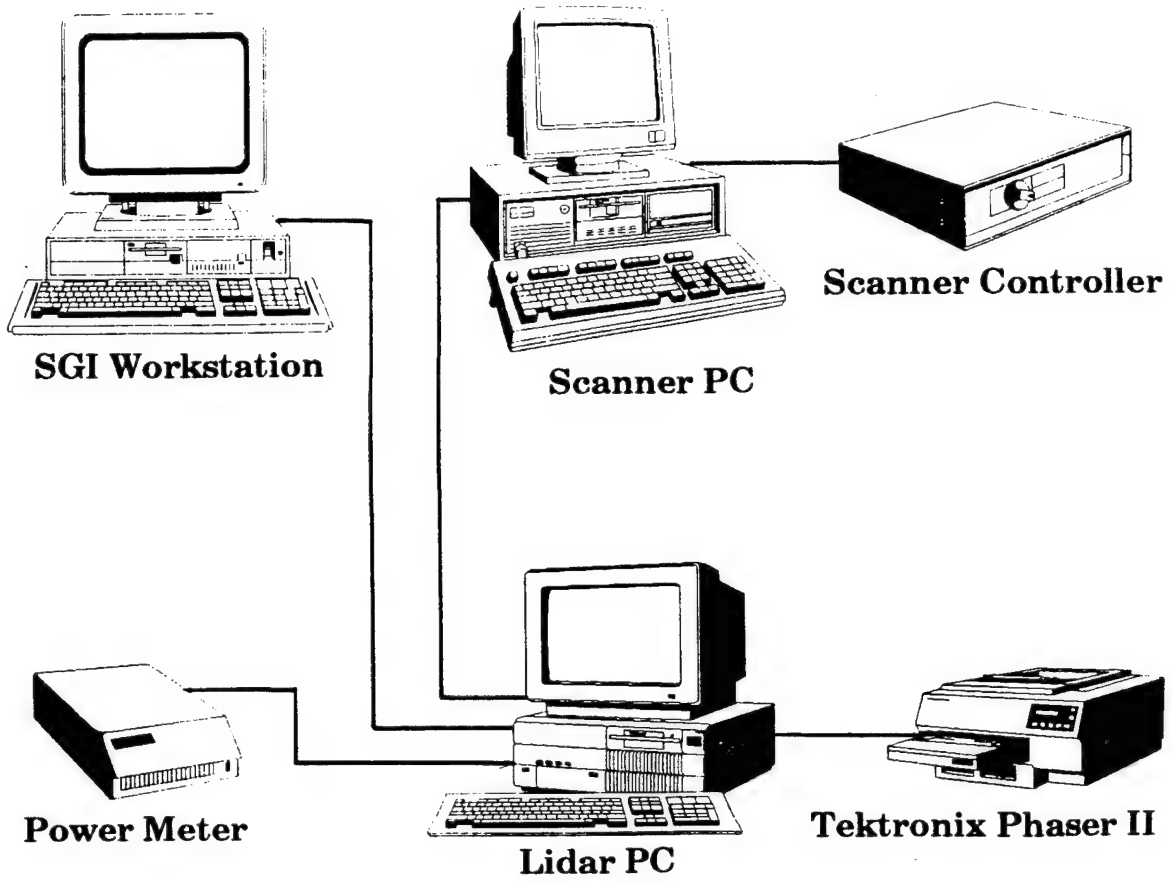

Figure 19. VIL computer interconnections during shipboard use.

Software Modifications

The software that runs on the "Lidar PC" had to be modified since it no longer controlled the scanning mechanism directly. The program was rewritten so that the scan angles could be sent out over the serial port at 19.2k baud to the "Scanner PC".

A program was written for the "Scanner PC" that reads the gyros, reads the scan angles from the "Lidar PC", calculates the coordinate transformations and controls the scanner motion. The flow chart in figure 20 depicts this procedure graphically. Appendix 12 lists the programs and gives descriptions of the program functions.

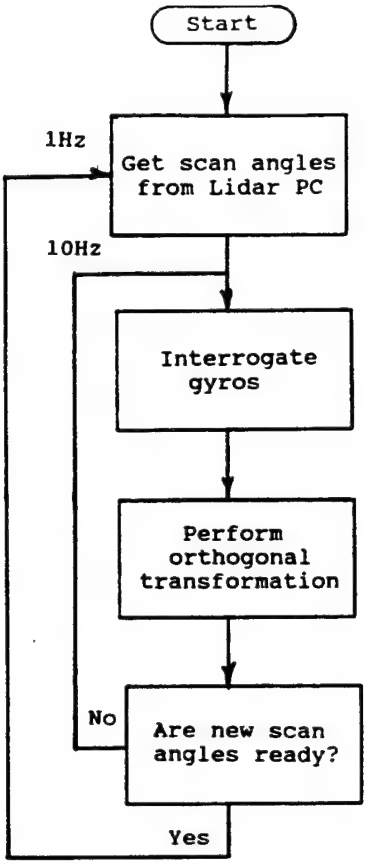

Figure 20. Order of events during the shipboard data acquisition cycle.

Safety Aboard Ship

The VIL scanning mechanism is limited by hard stops so the laser can not point in the direction of ship's personnel. The stops limit the scanning motion both in azimuth and elevation. An observer is located outside of the VIL shelter and monitors the surroundings. If a situation arises in which the laser could endanger anyone then it is immediately shut down with an external, hand-held KILL switch.

10. Airborne Use of the Lidar Equipment

The airborne lidar has the advantage of being highly mobile and can be operated over a wide, geographical-area in a reasonably short period of time. The lidar has been used in a non-scanning mode on Navy P-3 Orion aircraft several times and could be used in a scanning mode in the future. There are several software and hardware modifications that must be made when operating the lidar in an aircraft.

Purpose

The lidar has been flown on Navy P3 Orion aircraft to gather information about the marine boundary layer. During the Key90[10] experiment, flights were made over the Atlantic ocean south of the Florida Keys to obtain vertical profiles of atmospheric aerosol structure. This data was compared to insitu measurements made by NRL personnel on board the boat, RENEGADE, and with measurements made by NCCOSC personnel in the Navajo Piper Cub aircraft. Data gathered were used to test the Naval Oceanic Vertical Aerosol Model[11].

During the VOCAR experiment, held off the coast of California in 1992, the lidar was flown over sections of the Pacific ocean and measured boundary layer profiles. Estimations of atmospheric extinctions were made with the lidar returns. This data was also compared to insitu measurements made by the NCCOSC Navajo Piper Cub aircraft. Changes in boundary layer height and depth were measured.

Measurements could be made from an aircraft that would allow the use of a tomographic method[12] to objectively measure extinction and backscatter of the atmosphere with a single-wavelength, scanning lidar.

Aureole Lidar

Aureole lidar is a variation on the typical lidar and is used to obtain information from a down-looking lidar to estimate atmospheric extinction[13]. As shown in figure 21, two signals are measured by the down-looking lidar. The first is the lidar return indicated by the center, narrow field-of-view. The second is the aureole return and is the wider field-of-view in the figure. The aureole sensor looks at the light that has been scattered by aerosols back towards the sensor from the sea-surface reflection. The narrow field-of-view return provides a range resolved profile of backscatter and the wide field view provides a measure of forward scatter. Using the forward scatter signal (which is highly correlated with optical depth), a range resolved extinction profile is derived from the backscatter profile.

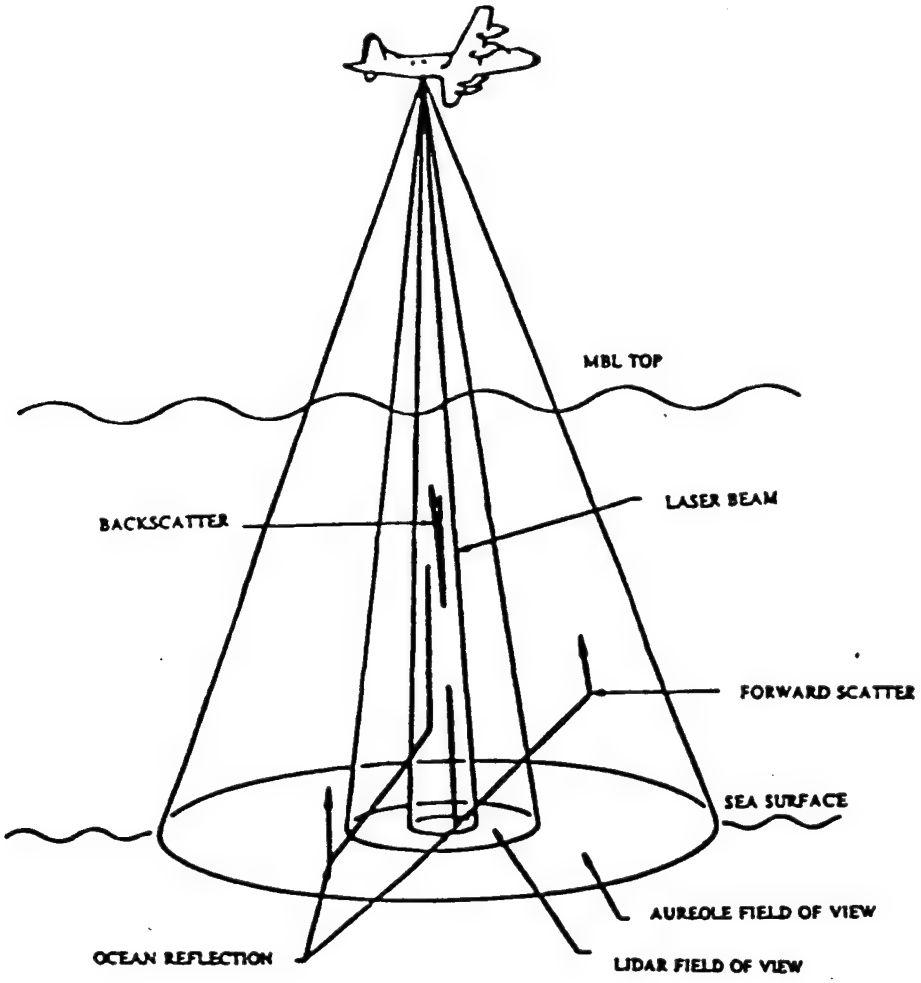

Figure 21. Signal paths of the lidar and aureole signal.

Hardware Modifications

Several modifications must be made to the lidar and to the aircraft for airborne operations aboard a P3 Orion. The airborne lidar system is pictured in figure 22 with the main components displayed. The rear access door of the P3 must be removed and a door, with a window made of 1" thick, optical-quality glass, must be re-installed. The lidar is mounted on a flat, aluminum frame that is bolted to the seat-rails of the aircraft. The laser, telescope, directional mirrors and sensors are mounted on the frame. The receiving mirror rests over a hole in the floor of the aircraft that is positioned over the window in the aft door that was replaced. For safety, the lidar pallet is then covered with a thin-walled aluminum box to prevent exposure to laser light in the aircraft cabin.

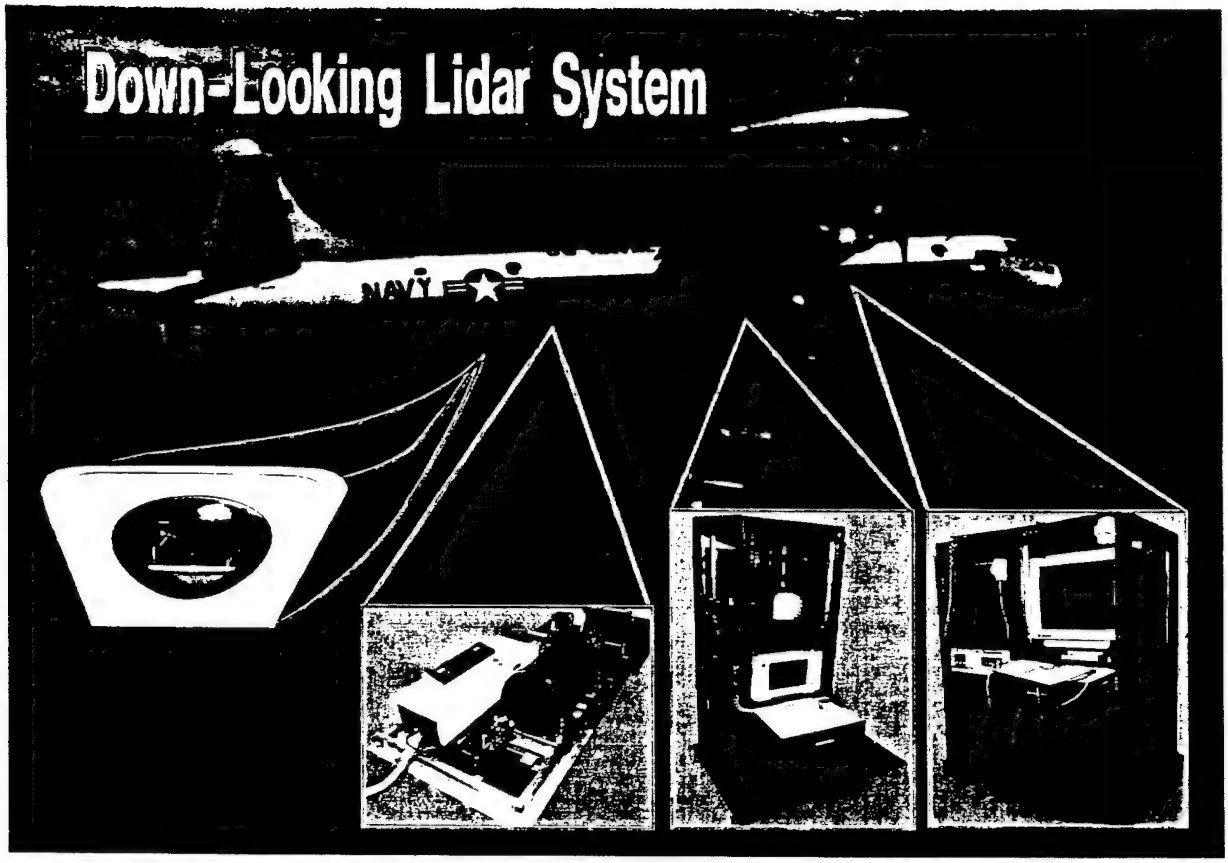

Figure 22. Airborne lidar system.

The laser beam leaves the laser, is redirected by two small mirrors through a tube and exits through the bottom of the aircraft through the aft-door window. The scattered-light follows the path of the laser beam back into the plane, reflects off the large mirror mounted at 45° and into the collecting mirror of the telescope.

The telescope has to be modified to make aureole measurements. The aureole signal sensor package, a Hamamatsu photomultiplier tube (PMT), must be installed in the telescope tube behind the telescope's secondary mirror. A Bertran high-voltage power supply provides excitation to the PMT.

Several CAMAC modules must be added to provide signal conditioning to the aureole signal. A TRANSIAC 6102 amplifier, a DSP 2001 digitizer, and a DSP4101 averaging memory module are used to obtain the aureole signal.

Software Modifications

The software must be modified to control the extra CAMAC modules and to store the aureole data. Appendix 12 has a list of the software, the machine it operates on and the software descriptions.

11. System Improvements

The VIL system hardware and software are continually being modified in an effort to improve system performance. The following suggestions are meant as a guide for further VIL development and improvement.

Increase Data Acquisition Speed

The VIL is presently limited by the DAT tape speed of 1Mb/s for data storage. If faster tape drives become available, or if optical technology becomes a less expensive storage alternative then those devices should be acquired. In the meantime, it may be desirable to use data compression algorithms during data acquisition to reduce the amount of tape space required.

Another limiting factor is the SCSI bus speed and bandwidth. The present bus used is known as SCSI-1 , which is the first SCSI iteration, and can sustain data transfers at about 5 Mb/s. The new SCSI-2 and SCSI-3 buses can transmit data at up to 20 Mb/s.

The present system uses the CAMAC bus for data acquisition. The VME bus is 32 bits wide and if coupled with an SGI Onyx system with built in VME bus the data acquisition speeds could be tripled.

Scanner Improvements

There are several improvements that could be made to the scanning system to improve performance and increase safety. Presently, the hard stops do not have any means of notifying the computer if they have been actuated. This means that the rotation stage that collided with the hard stop will continue to try to move until the operator removes power to the scanner. Indicator switches should be installed on the hard stops that automatically turn off scanner motion if a hard stop is reached.

Mirror Coatings

The large scanning mirrors should be resurfaced and coated to attain near 100% reflectivity at 1064 nm. The mirrors presently are only 60% efficient which means that only 15% of the total available return light is detected. The maximum detectable range would double if the coating were state of the art.

12. Acknowledgements

Funding for the VIL shelter was provided by the Office of Naval Research under Research and Technology grant # 43AB201-01. The authors wish to thank Mr. Bob Bluth of ONR for his continued support. The aircraft measurements made during the Key90 and VOCAR experiments were made for NRAD under the Program Element 62435N. The authors would like to thank Dr. Juergen Richter for his support. Some equipment described in this report was purchased by funding from Program Element 61153 (which is administered by NRL). We would also like to thank Tom Salvaille and others at Oceaneering Inc. for the excellent work done modifying the shelter.

REFERENCES

1. Collis, R.T.H., "Lidar", Advances in Geophysics, Eds. Landsberg, H.E. and J.S. Mieghem, Academic Press:New York (1969).

2. Measures, Raymond M., Laser Remote Sensing: Fundamentals and Applications, New York:Wiley (1984).

3. Sedgewick, Robert, Algorithms, Addison-Wesley:Reading, Mass, 99 (1983).

4. W.P. Hooper, "Aureole lidar: instrument design, data analysis, and comparison with "spectrographic measurements, Appl Opt. 32, 4019-4027 (1983).

5. Durkee, P.A. et al, "Monterey Area Shiptrack (MAST) Experiment Science Plan", Naval Post Graduate School Report NPS-MR-94-004,(1994).

6. James, Jeffrey E. and William P. Hooper, "Beam Pointing Stabilization for a Shipboard Volume Imaging Lidar", NRL Report Number , (1995).

7. Hooper, William P., J.E. James and R.J. Lind., "Lidar Observations of Turbulent Vortex "Shedding by an Isolated Topographic Feature, To be published 1995.

8. Blanc, Theodore V. and Reginald E. Larson, "Superstructure Flow Distortion Corrections for Wind Speed and Direction Measurements Made From NIMITZ Class (CVN68-CVN73) Ships", Naval Research Laboratory, NRL Memo Report NRL-9215 (1989).

9. Hooper, W. P. and E. W. Eloranta, "Lidar Measurements of Wind in the Planetary Boundary Layer: The Method, Accuracy and Results From Joint Measurements with Radiosonde and Kytoon", JCAM 25, 990-1001 (1986).

10. Gathman, S.G. et al, "NOVAM Evaluation Utilizing Electro-Optics and Meteorological Data from KEY-90", Technical Report 1608, September (1993).

11. Gathman, S.G. and K.L. Davidson, "The Navy Oceanic Vertical Aerosol Model", NCCOSC Technical Report 1634, December (1993).

12. Hooper, William P., "Using Lidar Tomography to Characterize Scattering in a Turbulent Media", Naval Research Laboratory NRL/MR/7220-94-7478 (1994).

13. Hooper, William P. and H.E. Gerber, "Down Looking Lidar Inversion Constrained by Ocean Reflection and Forward Scatter of Laser Light", Applied Optics, Vol. 25, 689, March (1986).

APPENDICES

APPENDIX 1. Statistical characterization of lidar data.

The marine boundary layer is formed and maintained by atmospheric structures. The larger of these structures are scaled by the boundary layer depth and are normally 1km to 100 m in size. Since a contrast in aerosol content and moisture exists between the air inside and outside these structures, the lidar can be used to observe these structures. The signal from these structures can be used to characterize the boundary layer and also the lidar data.
The return can be split into signal and noise components:

$$P_{ij} = \bar{\varsigma}_j + \varsigma_{ij} + \eta_{ij}, \tag{1-1}$$

where
i is time,
j is range,
$\bar{\varsigma}_j$ is the average signal component,
ς_{ij} is the variable signal component, and
η_{ij} is the noise component.

In equation (1-1), the combined signal components are:

$$\bar{\varsigma}_j + \varsigma_{ij} = \frac{K\beta_{ij}\exp^{-2\tau'_{ij}}}{r_j^2}. \tag{1-2}$$

If lidar data is being taken to observe the aerosol structures, then the average components are removed and the signal becomes the variable components.

For this analysis, the profiles are all assumed to be made with the lidar pointing in the same direction. Since noise can be caused by the transmitter (such as laser output energy variations) and receiver (such as limitations in response time), noise at different ranges in the same profile can be correlated. For this appendix, noise between profiles is assumed to be uncorrelated. This assumption is not always correct since time varying, strongly attenuating structures can add noise at ranges greater than the structures. The correlation between profiles separated in time is defined to be:

$$Corr_{1j} = \frac{\sum_{i=1}^{I}(P_{ij}-\bar{P}_j)(P_{i+1j}-\bar{P}_j)}{\left[\sum_{i=1}^{I}(P_{ij}-\bar{P}_j)\sum_{i=1}^{I}(P_{i+1j}-\bar{P}_j)\right]^{1/2}}, \tag{1-3}$$

where $corr_{1j}$ is the correlation between profiles at one range separated by one lag time and the overbar denotes a time average. In terms of signal and noise components, the correlation

becomes:

$$corr_{1j} = \frac{\overline{\varsigma_j^2}}{\overline{\varsigma_j^2} + \overline{\eta_j^2}}, \tag{1-4}$$

where the following assumptions are made:

(1) the average return is equal to the average signal component:

$$\overline{P_j} = \overline{\varsigma_j}, \tag{1-5}$$

(2) the product of signal and noise are neglected:

$$\sum_{i=1}^{I} \varsigma_{ij} \eta_{ij} = 0, \tag{1-6}$$

(3) the statistical difference between the two time series separated by one time lag is insignificant.

The signal to noise ratio becomes:

$$SNR_j = \frac{1}{\left[\frac{1}{corr_{1j}} - 1\right]^{1/2}}, \tag{1-7}$$

where the signal to noise ratio is defined to be:

$$SNR_j = \left[\frac{\overline{\varsigma^2}_j}{\overline{\eta^2}_j}\right]^{1/2}. \tag{1-8}$$

APPENDIX 2. Example of Outdoor Laser Range Firing Log

1. Command where firing occurs: _____

2. Range Location: _____

3. Date: _____

4. Laser System: _____

5. NRL Code: _____

6. Person In Charge: _____

Firing #	Time	Target Location	Firing Position/Heading
1.	_____	_____	
2.	_____	_____	
3.	_____	_____	
4.	_____	_____	
5.	_____	_____	
6.	_____	_____	
7.	_____	_____	
8.	_____	_____	
9.	_____	_____	

_____
SIGNATURE(Laser Safety Supervisor)

NOTE: To be used only when firing laser(s) outdoors.

NDW-NRL 5100/12101 (12-87)

APPENDIX 3. VIL Shelter Construction Drawings

SCALE : ½" = 1'-0"

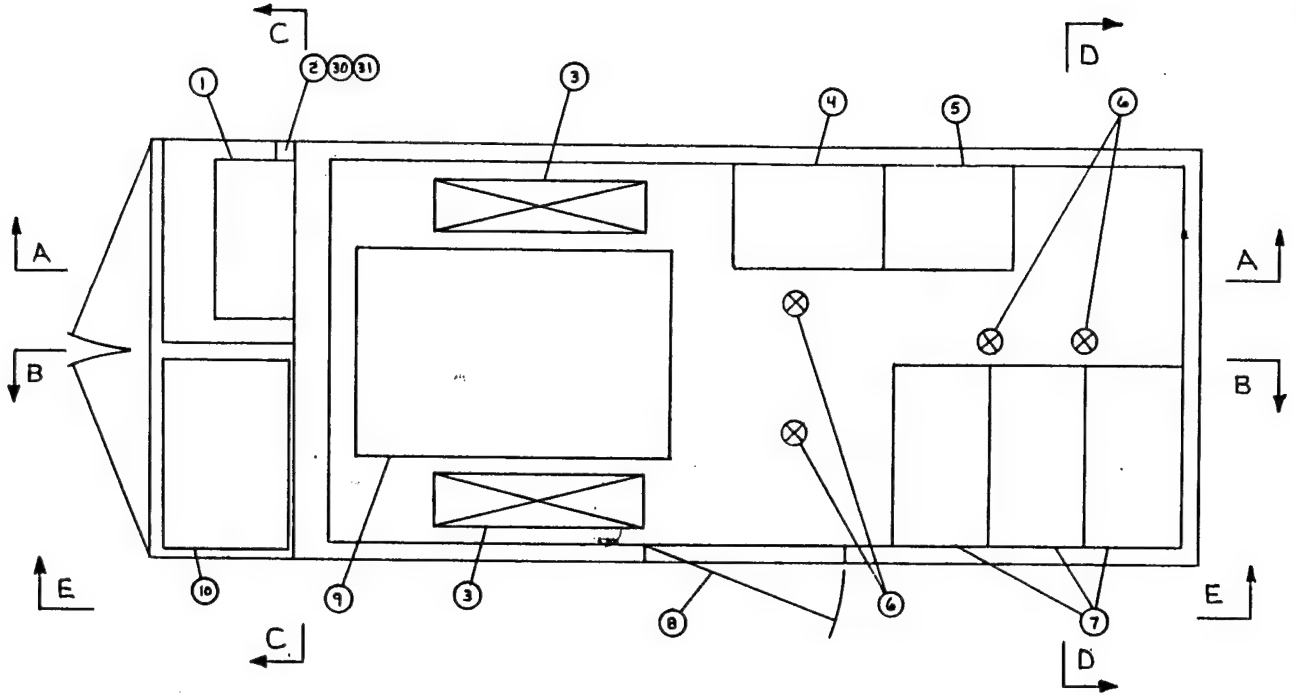

1. MARVAIR AC/HEAT UNIT
2. MAIN POWER RACEWAY
3. 2 BULB 1'x4' FLUORESCENT LIGHT
4. LASER POWER SUPPLY
5. LASER COOLER
6. FLUSH MOUNTED TOP HAT LIGHT
7. ELECTRONIC RACKS
8. 46" x 72" WATERTIGHT DOOR
9. LIDER PALLETE
10. LASER HEAT EXCHANGER
11. LASER MAIN POWER DISCONNECT
12. ELECTRICAL CIRCUIT PANEL
13. SLIDE MOUNTS
14. 110 V. RECEPTACLE
15. STORAGE AREA (OUTSIDE ACCESS)
16. AC/HEAT RETURN AIR
17. AC/HEAT SUPPLY AIR DEFLECTOR
18. UNISTRUT RAILS
19. RECESSED CABLE RACEWAY/OUTLET PORT
20. 50 AMP RECEPTACLE
21. 100 AMP RECEPTACLE
22. 25 AMP RECEPTACLE
23. LIGHT SWITCH W/DIMMER
24. AC/HEAT THERMOSTAT
25. FOLDING STEPS
26. WALL PHONE JACK
27. BASE PLATE (RACKS)
28. AC/HEAT VENTS
29. CEILING DECK PLATES
30. 220 3Φ 200 AMP FLANGED MALE HUBBLE
31. 220 3Φ 200 AMP FEMALE HUBBLE
32. 150 LOCK STAND
33. ENTRANCE DOOR STEP
34. PORCH LIGHT
35. PHONE/ELECTRONICS CONNECTIONS
36. SAFETY HANDLE
37. HATCH COVER
38. HATCH COVER TIE DOWN

- FLOOR MATTING
- PRIMER / PAINT

SHEET 1 OF 6

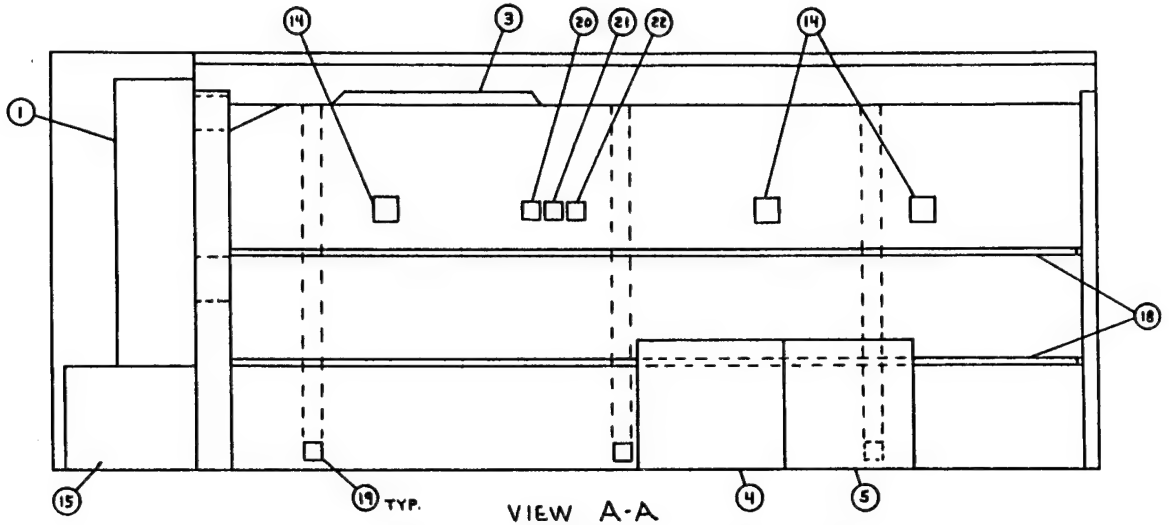

VIEW A-A

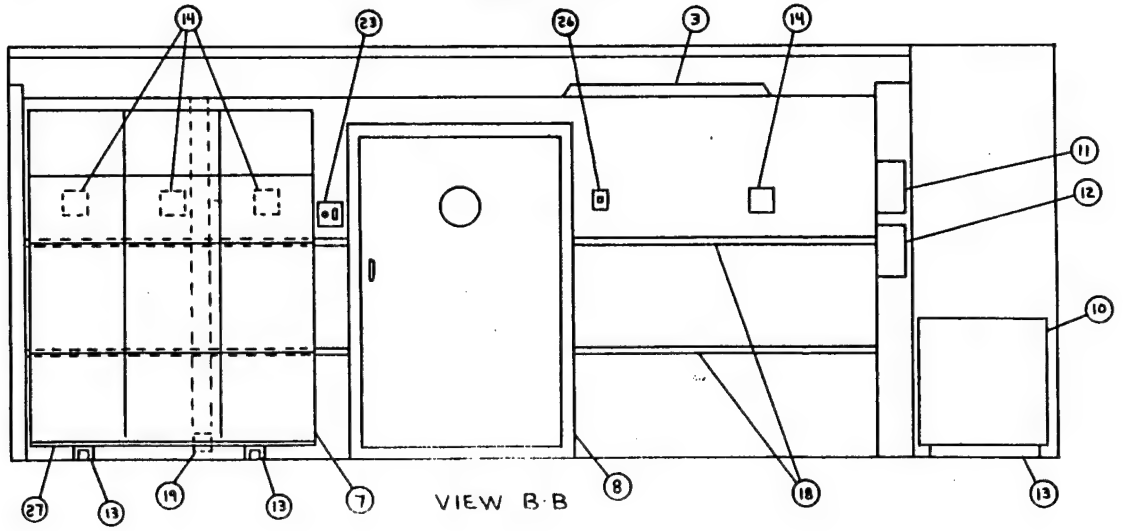

VIEW B-B

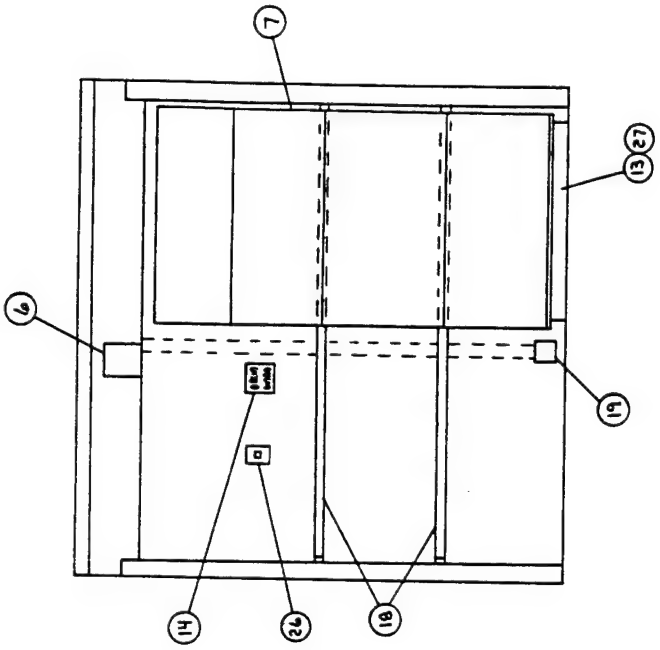

VIEW D-D

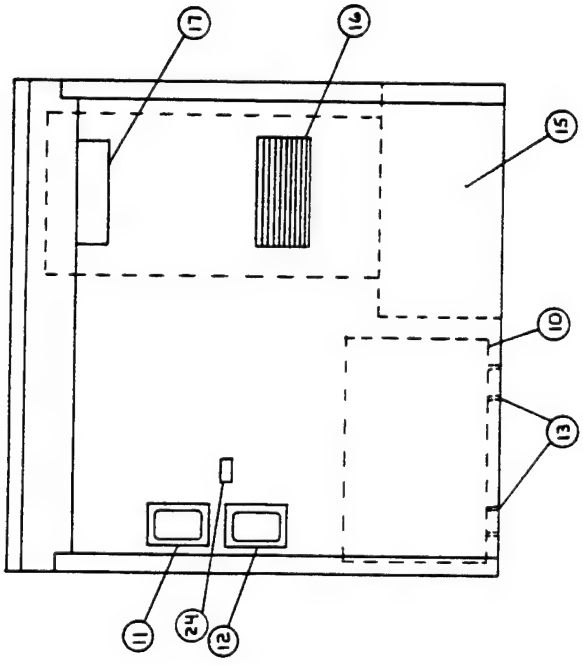

VIEW C-C

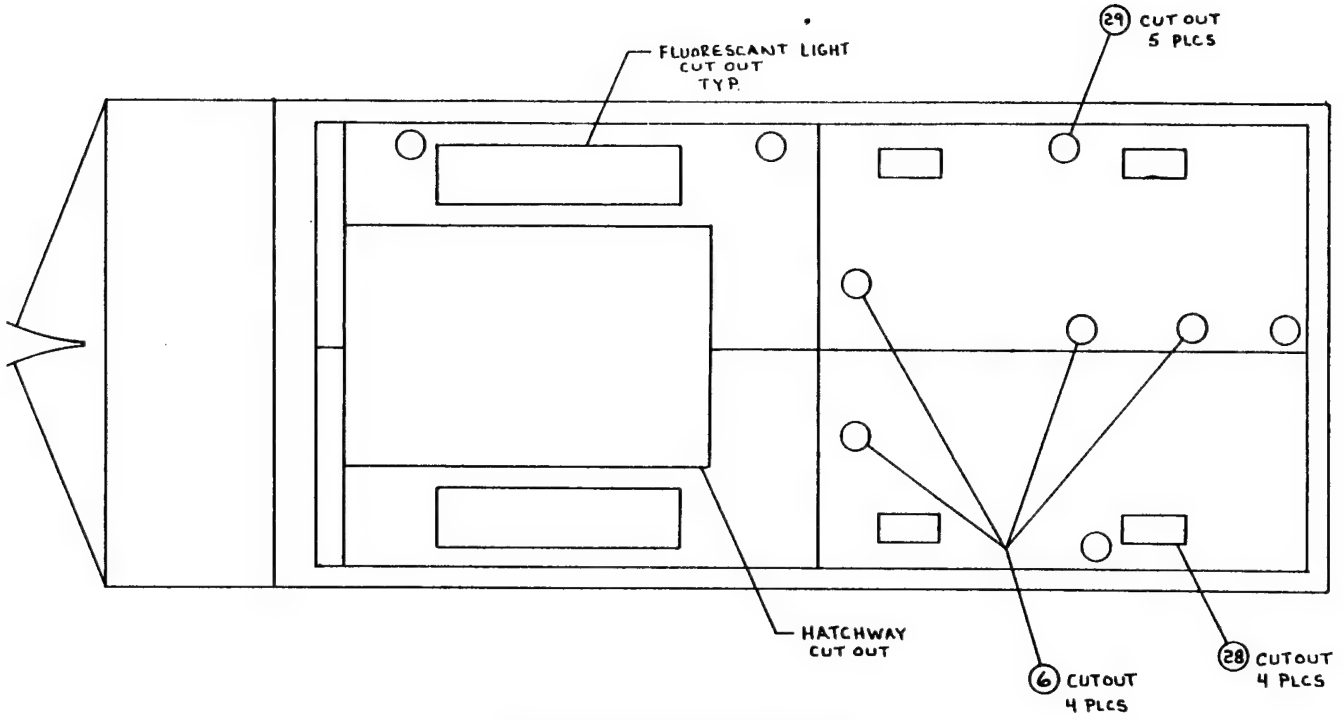

INTERIOR CEILING LAYOUT

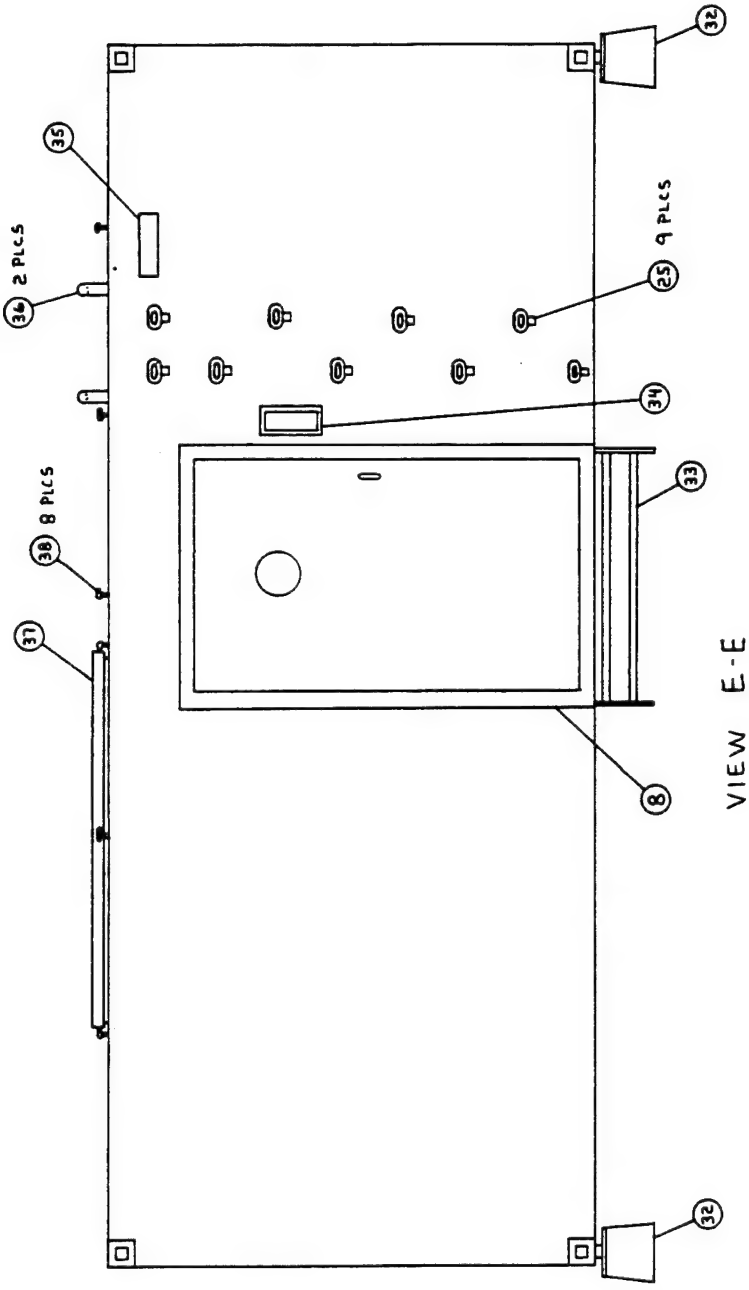

VIEW E-E

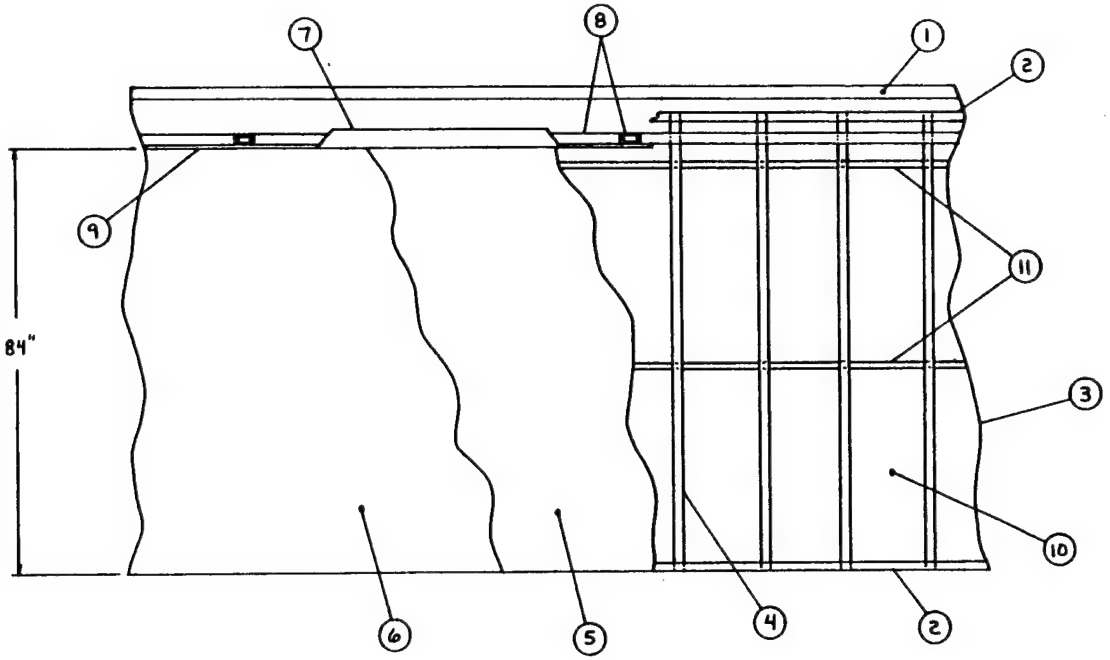

TYPICAL WALL SECTION

1. 2⅛" THICK BOARD INSULATION
2. 1⅝" STEEL WALL STUD TRACK
3. CONTAINER WALL
4. 1⅝" STEEL WALL STUD (WELDED TO CONTAINER WALL)
5. ½" WAFERBOARD PLYWOOD
6. ¼" THICK CARPET
7. 2 BULB 1'x4' FLUORESCENT LIGHT
8. 2"x3"x ⅛" WALL STEEL TUBE (WELDED TO CONTAINER WALL)
9. ¾" MELAMITE LAMINATED PLYWOOD (WHITE)
10. 3½" x 15" FIBERGLASS INSULATION.
11. 3" x ⅛" STL. FLAT BAR BRACING

APPENDIX 4. Access Panel Connector Pinouts

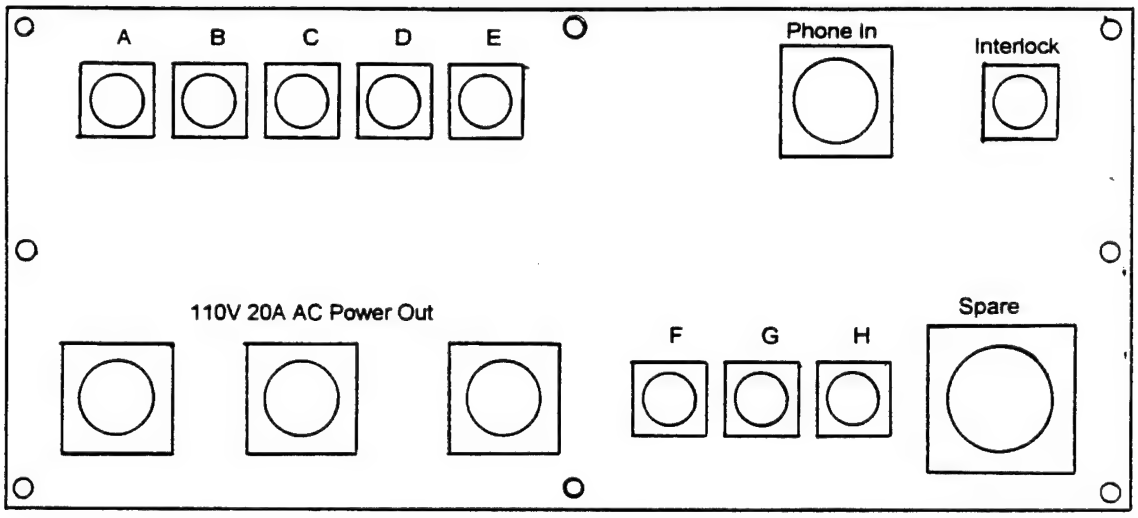

Figure 23. Access panel connector layout.

Coaxial BNC Connector A-D GPS Antenna Attachment
Coaxial BNC Connector E Magnetic Compass
Coaxial BNC Connector F-H Spare Analog Inputs

Bendix 10-98P 6-Pin Connector Phone Line In

A - Red
B - Green
C - Black
D - Yellow
E - NC
F - NC

Bendix 8-2P 2 Pin Connector External Laser Interlock

A - Interlock Out
B - Interlock Return

Bendix 14-5S 5 Pin Connector 110V/20A AC Out

A - AC Hot
B - AC Neutral
C - Ground
D - NC
E - NC

Bendix 12-8P 8 Pin Connector Spare

No Connections

APPENDIX 5. DMA, Interrupts, and Addresses of the 486 PC

PC Slot	Function	Board Name	Int #	Base	DMA
1 MM2000	Scanner Cont.	MM2000	5	240H	NA
2 VGA	VGA Graphics	VGA	-		NA
3 Adaptec	SCSI Cont.	1542B (SCSIA)	15	330H	5
4 Adaptec	SCSI Cont.	1542B (SCSIB)	11	334H	6
5 COM 3,4	Spare	NA			NA
6 COM 1	Mouse	NA			NA
7 COM 2	Energy Monitor	NA			NA

APPENDIX 6. VIL System Alignment Procedure

In order for the lidar to operate properly, the optics must be aligned. This means the laser beam that passes into the atmosphere must point in the same direction that the recieving telescope does, to an accuracy of about 1 micro radian. Also, the sensor must be positioned in the focal plane of the telescope and be aligned with the focal point in that plane. Please refer to figure 9 for the following description.

Note: All alignment procedures should be performed wearing proper eye protection when necessary. The beam is invisible to the human eye so fluorescing IR cards and an IR Finder Scope are necessary to perform the alignment.

1. The first step in the alignment procedure is to adjust the large mirrors in the scanning mechanism to approximately 45° to the plane of the rotation stages. This can be done by simply loosening the adjustment bolts on the mirror frames and using a 45° triangle to align the mirror to the proper angle. Tighten the bolts once the mirrors have been properly positioned.

2. The laser beam must be traced from the laser head to the first transmission mirror (M1) using a fluorescing card. The position of this mirror should be adjusted so the laser beam falls in its center. M1 should be at approximately 45°.

3. Adjust the power meter (PM1) so the beam passes freely through it without hitting any edges.

4. Adjust the second transmission mirror (M2) to approximately the same position as M1. It should be directly above M1 and angled at 45°.

5. Adjust the angular position of M2 so the laser beam falls in the center of M3.

6. Adjust M2 vertically so the laser beam falls on M3.

7. Adjust the angular position of M2 so the beam falls in the center of M3.

8. Place the centering rods (CR1 and CR2) in place on the horizontal stage opening and the vertical exterior surface of the elevation stage. The centering rods are simply metal or wooden rods that have the center drilled out (1/2" dia) for the laser beam to pass through.

9. Adjust M3 so the laser beam passes through the hole in CR1, reflects off the first large mirror (M4), reflects off the second large mirror (M5), and passes through the hole in CR2. This will ensure that the beam is coaxially positioned with the recieving optics at the point of transmission.

10 . Next, a rough alignment is done by pointing the scanning mechanism at a low power laser

a few hundred meters away.

11. The low power laser (HeNe or low power IR) is mounted on a tripod and is positioned by screw adjusters. The laser is pointed at the scanner and then the scanner is adjusted so the laser beam falls directly on the opening of the elevation stage.

12. The telescope is now adjusted to get the focus as close as possible to the sensor.

13. Once this has been accomplished, the low power laser is replaced with a corner reflector. Then the laser transmitter from the lidar is turned on and adjusted by way of M2 and M3 so the beam falls right on the corner reflector. Note: Cover the sensor during this part of the alignment. Use the IR finder Scope to view the return.

14. The lidar is now in a rough alignment. To get the final alignment it is necessary to aim the beam several km away.

15. At CBD, the lidar is aimed at the Tilghman Island tower. The top of the tower is detected either by monitoring the return from the laser or from an observer located at Tilghman Island.

16. A low-power laser (Continuous, 35 mw, 1.06 um, diode-pumped) is aimed back towards the VIL shelter and positioned onto the scanning mirror M5. Make sure that the sensor is covered so the low-power laser does not damage it.

17. The low power laser light is then focused onto the covered sensor. Adjust the position of the sensor so the return light is focused on the sensitive area of the sensor.

18. The VIL should now be in alignment.

APPENDIX 7. Reference Manuals for the Volume Imaging Lidar.

Silicon Graphics Workstation Manuals

GL Manuals
SGI C Reference Manuals
IRIX Device Driver Programming Guide
Document # 007-0911-020 SGI (1992)
Python DDS and DDS-DC DAT Tape Drives and Autoloaders SCSI Manual
PN 27298-001 Archive Corp. (1992)
C - The Complete Reference, By Schildt, McGraw-Hill

486 PC Manuals

DOS and System manuals for 486 DX2 PC
Adaptec 1542B Technical SCSI Manual

CAMAC Crate Module Manuals

Transiac 2010/2012 Operators Manual, Waveform Digitizer (1983)
DSP Model 2001 Transient Recorder 100Mhz, 8 Bit.
Transiac Model 4100 Averaging Signal Memory
DSP Model 4101 Reference Manual (1988)
Transiac Model 1020 Differential Amplifier
Kinetic Systems Corp. Model 3929-Z1B SCSI Crate Controller Instruction Manual,
MN 000118

Scanner Manuals

Klinger Motion Master 2000 Quick Installation and Setup Guide Rev 2.3
Klinger Motion Master 2000 Users Manual Rev. 2.2

Laser Manuals

Continuum Operator and Maintenence Manual, Mach 500 Laser COM 160 (1991)
Spectraphysics Quanta Ray DCR2A Pulsed Nd:Yag Laser Instruction Manual,
PN 230000-106A
Molectron Detector J25/J50 Pyro Electric Joulemeter Operators Manual (1987)

APPENDIX 8. VIL Data Records

The data record sent from the 486 PC to the SGI workstation consists of a 512 byte header block and usually a 16 Kbyte data block.

Header block format:

Byte 1-4: A value that indicates the version of software and data set. Presently set to 0,0,241,217.

Byte 5-8: Shot number, Byte 5=LSB, Byte 8=MSB

Byte 9-12: H,M,S,Frac

Byte 13-15: Month, Day, Year

Byte 16-19: Elevation Angle, Byte 16=LSB, Byte 19=MSB

Byte 20-23: Azimuth Angle, Byte 20=LSB, Byte 23=MSB

Byte 24: Not Used

Byte 25-26: Length of data buffer (16K)

Byte 27-28: Switch Settings of CAMAC 2010 Module

Byte 29-30: Length of data from energy monitor

Byte 31-34: Azimuth with offset (if any)

Byte 35-38: Elevation with offset (if any)

Byte 39: Number of waveforms averaged by 4100

Byte 40-512: Energy monitor data

Data Block Format:

4 bytes per range bin (Usually 4096 range bins)

APPENDIX 9. Descriptions of the VIL Software

ACQUIRE.C

This is the main software that runs on the SGI system. It reads data from the "Lidar PC" over the SCSI bus, stores data on DAT tape and display the return in several types of windows. Windows include Range-Time Indicator (RTI), Range-Height Indicator (RHI), Plan-Position Indicator (PPI), Oscilloscope, 3D, Fixed-Range Indicator (FRI), Wind Speed and Turbulence.

DSLIB.C

This is an object file linked with the ACQUIRE.C program that controls the SCSI bus. It contains the code for all the SCSI commands that are allowed on the bus.

DSLIB.H

This header file includes definitions regarding the SCSI Controller and functions related to it.

GL.H

Header file that supports the GL library of functions.

GL_SLIB.C

A library of functions used to control the graphics hardware and the graphics appearance.

GL/DEVICE.H - A header file that includes definitions for graphics devices.

486 PC Operating Software

VIL.PAS

This is the main system software and controls the CAMAC crate, reads the laser power monitor, controls the scanning mechanism, and sends data to the SGI for storage. It operates on the "Lidar PC" in a DOS environment. Scanner limits and angles can be changed using a mouse as input. There are several parameters that must match the settings in the ACQUIRE.C software that operates on the SGI. They include NUM_BYTES, MAXBYTES, ??

MOUSESCAN.INC

This include file contains everything needed to operate and control the scanning mechanism. It interfaces with the Klinger MM2000 stepper controller. It allows interrupt-driven positioning

on the scanning mechanism.

SCSI.INC

This file includes all the functions, definitions, and procedures necessary to operate the SCSI bus. It allows multiple SCSI controllers in the PC. Controls data transfers, SCSI bus testing, etc. Uses target mode operation to communicate with CAMAC and SGI. Adaptec 1542A and 1542B SCSI controllers are used in the 486 PC. Note: The 1542C SCSI controller made by Adaptec does not work properly in target mode and therefore does not work in the VIL system. Use only 1542A and 1542B SCSI controllers.

PWRMETER.PAS

This file enables use of the JD501 power meter and the RS232 serial port. It contains routines for handling serial port interrupts, setting baud rates, and other serial port parameters. Multiple ports can be used simultaneously.

TRAKBALL.TPU

This TPU file contains the procedures and functions required to use a trakball or mouse with the VIL system. It has routines for reading the mouse position, button clicks, and whether or not a button has been pressed.

The previous working version of the system was VIL5.PAS and used SCANNER.PAS instead of MOUSSCAN.PAS. It did not use TRAKBALL.TPU. This version used the keyboard for adjusting parameters for lidar operation.

APPENDIX 10. VIL System Maintenance

The lidar does not require much maintenance, but the following items are recommended as needed.

Clean Mirrors Within the Shelter

Clean mirror surfaces. Use a can of pressurized air or a camel hair brush to remove any loose contaminants. Using lens tissues or cotton, clean the mirrors with a solution made of 1/3 isopropyl alcohol, 2/3 distilled water, and two drops of biodegradable liquid dish detergent per each quart of solution (Soap by itself will leave a film).

Clean Scanner Mirrors

The large scanner mirrors can be cleaned by spraying distilled water on them and letting the water run off and evaporate. If a more thorough cleansing is required then use the solution described above and gently rub with lens tissues. The scanner covers may have to be removed. Care should be taken not to let the water drip onto the optics and electronics below the scanning mirrors.

Anti-rust Treatment

The scanning mechanism is made of hardened-steel and aluminum. The metal parts should be coated with silicone grease to protect them from corrosion and rust. Spray the silicone onto a rag and wipe it over the metal surfaces every few months to extend the life of the scanning mechanism.

The outside of the shelter should be washed periodically to remove contaminants that could damage the exterior. Make sure that any rust that appears is removed and the area repainted.

APPENDIX 11. Descriptions of the Shipboard VIL Software

The software associated with the shipboard lidar is listed below.

ACQUIRE.C

This program runs on the SGI workstation and is identical to the version for the ground based system.

SHIPMTR.PAS

This program runs on the "Lidar PC" and is the main program. It controls operation of the CAMAC crate, allows the user to adjust scanning and operating parameters, monitors the laser power meter, and sends scan angles to the "Scanner PC". It also adds header information to the returns and transfers the data to the SGI.

SHIPMTR.INC

This include file contains parts of the file "SCANNER.INC" (described earlier) and has been modified for shipboard use. Contains functions and procedures associated with the selection of scan angle parameters. This is part of the "Lidar PC" software.

SCSI.INC

This includes all the drivers and supporting functions and procedures to control the SCSI bus instrumentation including the CAMAC and SGI data transfers. Part of the "Lidar PC" software set.

PWRMTR.INC

Includes all RS232 functions and procedures to control the laser power meter and data transfers between the "Lidar PC" and the "Scanner PC". This is part of the "Lidar PC" software.

RATESCAN.PAS

This is the main scanner program. It runs on the "Scanner PC" and calculates orthogonal-transformations and controls the positioning of the scanner.

RATESCAN.INC

This is an "include file" that contains all the scanner functions and procedures to control the scanner. This is part of the "Scanner PC" software set.

APPENDIX 12. Descriptions of the Airborne Lidar Software

P3ACQUIRE.C

This program runs on the SGI and controls the storage of data onto DAT tape and the display of data. An RTI window displays the data in a rising-raster scan. This is very similar to the ACQUIRE.C software version used in the ground-based system but it has been modified to store and display the extra data from the aureole sensor. This is the software that operates on the SGI.

P3VIL.PAS

This is the main program which runs on the 486 PC. It controls the initialization and operation of the CAMAC modules. Reads aureole and lidar data and transfers to SGI for display and storage. This software runs on the 486 PC.

FASTVIL.PAS

P3_ACQ2.PAS, P3_LIDAR.PAS

These programs were written to control the data acquisition and display aboard the P3 when a failure of the SGI occurred. Data is stored on a tape drive in the 486 PC and displayed on the VGA display of the 486 PC.

P3SCSI.INC

This includes all the functions and procedures necessary to operate and control the SCSI bus and the devices attached to it. It is almost identical to the file SCSI.INC but has been modified to allow for the aureole data. This is part of the 486 PC software set.

POWRMTR.INC

This file includes the functions and procedures to control the power meter and the serial port. It is used on the 486 PC.

APPENDIX 12. Detector Calibration

The typical lidar return waveform decreases in strength by 10^{-5} as compared to the original laser-pulse power level. Both the range squared signal decrease and attenuation can cause these changes. For example, in a homogeneous atmosphere the signal decreases by 4 decades between 100 m and 10 km in range. Clouds cause similar changes in shorter distances (~100 m). A logarithmic amplifier is used to compress the range of signal changes. The sensor and logarithmic amplifier need to be calibrated, since the logarithmic scale factor can change with time and is sensitive to the overall alignment of the lidar.

The alignment is done at CBD using the tower as a topographic target and using a set of pre-calibrated neutral density filters to vary the signal. The logarithmic form of the lidar equation is:

$$S = \log_a[P\ R^2] = \log_a[K]+\log_a[\beta]-\frac{2\tau}{\ln[a]}+\log_a[1+n]\ , \qquad (12\text{-}1)$$

The return from a topographic target is:

$$S_0 = \log_a[K]+\log_a[\beta_0]-\frac{2\tau}{\ln[a]}+\log_a[1+n]\ , \qquad (12\text{-}2)$$

where S_o and β_o are the target lidar return and backscatter respectively. With a neutral density filter $[N_d]$, the return is:

$$S_{nd} = \log_a[K]+\log_a[\beta_0]-\frac{N_d}{\ln[a]}\ -\frac{2\tau}{\ln[a]}+\log_a[1+n]\ , \qquad (12\text{-}3)$$

Assuming that the system constants and optical depth are constant and ignoring the noise term, the difference between the two returns is:

$$S_{nd}-S_o = -\frac{N_d}{a}\ . \qquad (12\text{-}4)$$

Figure 26 shows the relationship between return strength and value of the neutral density filter for the three different topographic targets. The three curves are normalized by the return with a neutral density of 0.2. (The strongest return for the solid curve (with no neutral density) shows an unexplained non-linearity.) As the strength of each return is reduced by filters, the returns reach a noise threshold, where the noise component dominates. The strongest return is fit using a least squares algorithm to find the best estimate of the logarithmic amplifier constant (in this case a=454).

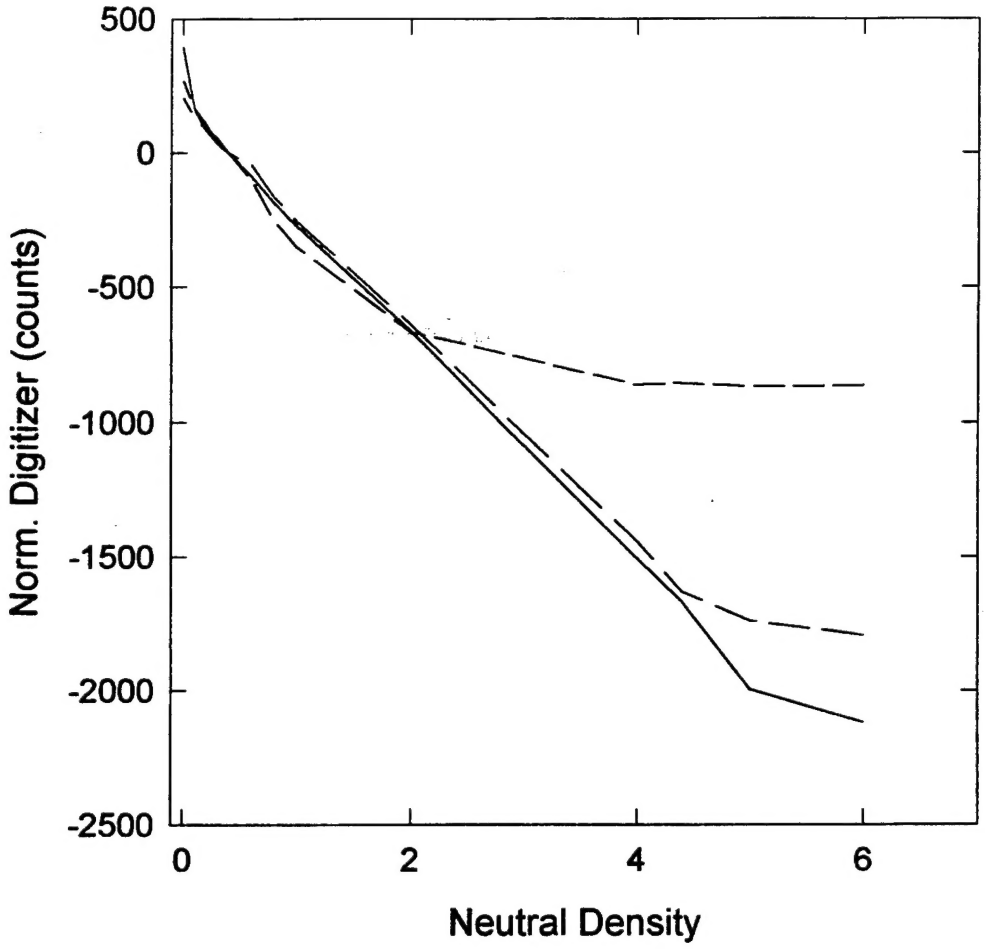

Figure 26. The relationship between digitizer counts and neutral density filter is shown. Curves for three topographic targets are plotted. The strength of the topographic targets are from strongest to weakest, using line types of solid, long dash, and short dash, respectively. The curves are normalized by a neutral density filter of 0.2 and the counts are therefore negative.

APPENDIX 13. Calibration of Azimuth and Elevation Angles

Both azimuth and elevation angles must be calibrated at fixed shore sites and even with gyro stabilization, the relative angles between gyros and scanning mechanism must be calibrated. While the VIL shelter can sometimes be leveled, calibrating the azimuth and elevation angles is quicker and more accurate. One of two methods can be used; either three or more stationary, hard targets are found or sea surface return can be used. The range and scanner angles for each target are determined. The maximum azimuthal separation should be at least 90° . The elevation angle can be derived from:

$$\cos(\phi'') = \sin(\theta)\cos(\theta_t)+\cos(\theta)\sin(\theta_t)\cos(\phi-\phi_{amt}) , \qquad (13\text{-}1)$$

where ϕ'' is the actual elevation angle (with respect to the Earth's surface), θ is scanner elevation angle, θ_t is the maximum elevation tilt angle, ϕ is azimuth angle, and ϕ_{amt} is the azimuth angle to the axis of minimum tilt. With the cosine, the range from the lidar to a target can be estimated:

$$R_{est} = R_e\cos(\phi'')+\left[R_e\left(R_e\cos(\phi'')-2\,(Z_o - Z_{oo})\right)\right]^{1/2} , \qquad (13\text{-}2)$$

where Z_o and Z_{oo} are the height of the scanning mechanism and target respectively and R_e is the Earth's radius. While scanner angles are known, the maximum tilt angle and the axis of this tilt is unknown. In the case of three targets, the two unknowns (maximum tilt angle and axis of minimum tilt) can be calculated; normally, however a series of targets are used. In this case, these angles can be found by minimizing the difference between the actual range and estimated range to targets using a Marquart algorithm:

$$\sigma_r = \sum_{i=0}^{N}\left[r - r_{est}(\phi_t,\theta_t,\theta_{amt})\right]^2 \qquad (13\text{-}3)$$

where σ_r is the rms difference between the measured and estimated ranges. (This algorithm can also be used to calibrate the elevation stage angles.) These angles are provided to a transform in the computer that controls the scanning mechanism. (At this point the angle can be easily checked and corrected if necessary). This corrects for the tilt of the scanning mechanism. Now using the azimuth angles to known targets, the scanner azimuth angle can be corrected by a simple azimuthal offset. (Using a topographic map, the lidar location can also be found.) Since refraction can significantly influence this alignment, the time of calibration needs to be carefully chosen to minimize this error. (The angle corrections can also be done automatically using a three axis GPS receiver.)